CFD Model Estimates of the Airflow Distortion over Research Ships and the Impact on Momentum Flux Measurements

M. J. YELLAND AND B. I. MOAT

James Rennell Division for Ocean Circulation and Climate, Southampton Oceanography Centre, Southampton, United Kingdom

R. W. PASCAL

Ocean Engineering Division, Southampton Oceanography Centre, Southampton, United Kingdom

D. I. BERRY

James Rennell Division for Ocean Circulation and Climate, Southampton Oceanography Centre, Southampton, United Kingdom

(Manuscript received 13 December 2001, in final form 17 March 2002)

ABSTRACT

Wind velocity and air–sea turbulent flux measurements made from shipborne instruments are biased due to the effect of the ship on the flow of air to the instruments. The presence of the ship causes the airflow to a particular instrument site to be either accelerated or decelerated, displaced vertically, and sometimes deflected slightly in the horizontal. Although recognized for some time, it is only recently that the problem has been addressed using three-dimensional computational fluid dynamics (CFD) models to simulate the flow over particular ships, quantify the effects of flow distortion, and hence correct the ship-based measurements. It has previously been shown that this improves the calculated momentum fluxes by removing disparities between data from different ships, or from instruments in different locations on the same ship.

This paper provides validation of the CFD model simulations. Two research ships were instrumented with multiple anemometers located in both well-exposed and badly exposed sites. Data are compared to the results of model simulations of the flow at various relative wind directions and wind speeds. Except when the anemometers are in the wake of an upwind obstruction, the model and the in situ wind speed estimates typically agree to within 2%.

Direct validation of the model-derived estimates of the vertical displacement of the flow was not possible due to the extreme difficulty of obtaining such measurements in the field. In this study, simulations of flows at 0° and 90° from the bow of the ship were made and displacements of about 1 and 5 m were found, respectively. These results were used to correct the in situ momentum flux data. In one case, the application of the different bow-on and beam-on corrections for vertical displacement successfully removed the disparity seen in the uncorrected data. In a second case, the beam-on vertical displacement overcorrected the flux results. This overcorrection could be caused either by uncertainties in the in situ estimate of the relative wind direction or by partial adjustment of the turbulence during the vertical displacement.

The effects of flow distortion are found to vary only slightly with wind speed, but are very sensitive to the relative wind direction and, if uncorrected, can cause large biases in ship-based meteorological measurements (up to 60% for the drag coefficient). Model results are given for bow-on flows over 11 research ships (American, British, Canadian, French, and German).

1. Introduction

The flow of air to ship-mounted instruments is distorted by the presence of the ship itself. This causes biases in both the mean wind speed estimate and in the measurement of the turbulent air–sea fluxes. While the problem of flow distortion has been recognized for many years (Hunt 1973; Wucknitz 1980; Dobson 1981; Blanc 1986, 1987), relatively few attempts have been made to quantify its impact at particular anemometer sites on individual ships. For example, Surry et al. (1989) and Thiebaux (1990) performed wind tunnel studies of the flow over the Canadian ships *Hudson* and *Dawson,* and found that, for a flow directly on to the ships' bows, anemometers mounted on a mast on the foredeck experienced flows that had both been decelerated by 1%, while the ships' anemometers that were mounted above the bridge experienced flows that had been accelerated by 6% and 7%, respectively.

Wind tunnel studies are costly and time-consuming

Corresponding author address: Dr. M. J. Yelland, James Rennell Division, Southampton Oceanography Centre, Empress Dock, Southampton SO14 3ZH, United Kingdom.
E-mail: mjy@soc.soton.ac.uk

to perform, and are limited by the wind tunnel speed and the physical size of the model. In recent years numerical modeling has been employed in order to simulate the airflow over ships (Kahma and Leppäranta 1981; Yelland et al. 1998; Dupuis et al. 2002, hereafter DGH). Kahma and Leppäranta (1981) used a simple two-dimensional potential flow model and found the flow at an anemometer on the main mast to be accelerated by 15% for bow-on flows. Yelland et al. (1998) (hereafter YT98) used a three-dimensional computational fluid dynamics (CFD) model to simulate a bow-on flow over the two ships, the RRS *Discovery* and RRS *Charles Darwin,* and used the model results to correct their inertial dissipation measurements of the drag coefficient. These authors presented some initial validation of the CFD models by modeling the CSS *Hudson* and CSS *Dawson* for flows on to the bow and found similar (within 2%) results to the earlier wind tunnel studies. However, this exercise provided limited validation data since (i) the acceleration of the flow was small at the sites examined, (ii) the wind tunnel studies provided no information about the vertical displacement of the flow, and (iii) the number of data was very small. More recently, DGH modeled the flow around the research ship *L'Atalante* for various relative wind directions and wind speeds and used the resulting estimates of the error in the measured wind speed to correct their inertial dissipation measurements of the heat and momentum fluxes. However, due to the small computational domain or ''wind tunnel'' used in their study, these authors were not able to accurately quantify the vertical displacement of the flow and relied mainly on the improvement in the resulting drag coefficient to wind speed relationship to provide indirect validation of their modeling results.

This paper attempts to provide more thorough validation of the CFD model simulations. To this end, the research ships RRS *Discovery* and the RRS *Charles Darwin* were each instrumented with up to 11 anemometers located at various sites around the ship. Some sites were expected to be well-exposed for winds from ahead and experience relatively small flow distortion, whereas other badly exposed sites were chosen in order to measure a more severely distorted flow. The instruments used, their locations, and the resulting data are described briefly in section 2. CFD models of both ships were made for flows at $\pm 30°$ to the bow, $\pm 15°$ to the bow and bow-on. Section 3 gives a brief description of the CFD models of the two ships.

Section 4 compares the in situ wind speed measurements with the CFD model results. It was not feasible to locate an anemometer far enough from the ship to be certain of measuring the completely undistorted or ''freestream'' flow, for example, by using a buoy-mounted anemometer. Thus it was not possible to obtain an in situ estimate of the absolute wind speed error caused by the flow distortion at a particular site on the ship. Instead, ''relative differences'' between data from pairs of anemometers are used.

In addition to being accelerated (or decelerated), the flow of air is also displaced vertically and may by deflected slightly in the horizontal. Absolute validation of the CFD-derived estimates of the vertical displacement of the flow is hampered by the extreme difficulty of obtaining such measurements in the field. However, indirect validation of this aspect of the CFD model results is presented in section 5. This section examines drag coefficient data sets that were obtained from two ships that experienced flow that had been displaced by about 1 m for flows directly over the bows of the ship and by 4 to 5 m for winds at 90° to the bow. Application of the model estimates of the vertical displacement of the flow to these in situ data removes or reduces the systematic disparity seen in the uncorrected results.

Section 6 examines the variation of the flow distortion with incident relative wind speed, using data from three ships that were modeled for bow-on flows at more than one wind speed. The in situ relative wind speed differences are used to validate the model results, which suggest that the effect of flow distortion on the measured wind speed is not significantly dependent on the incident wind speed.

During recent years the flow over a number of research ships has been modeled. The CFD-derived estimates of the absolute wind speed error and the vertical displacement of the flow for each ship are presented in section 7, along with the particular instrument locations examined. It is hoped that these data will be useful to researchers who have obtained meteorological measurements from these ships in the past, or to those making comparisons between ship- and buoy-based systems. The impact of flow distortion on the measured momentum flux is discussed for a ''typical'' instrument location in section 8.

2. The in situ wind speed measurements

a. Instrumentation

The instruments used during the *Darwin* and the *Discovery* cruises were Solent Sonic Research anemometers ($<1\%$ rms), Young AQ propeller vanes (± 0.2 m s^{-1}), Windmaster sonic anemometers (1.5% for winds below 20 m s^{-1}), and Vector cup anemometers ($\pm 2\%$). The figures in brackets give the instrument accuracy as specified by the manufacturers for the first three anemometer types. The Vector anemometers were calibrated by the Institute of Oceanographic Sciences (IOS) staff in the Met Office wind tunnel at Bracknell for a wind speed range of 1 to 34 m s^{-1}.

The RRS *Charles Darwin* was equipped with 11 anemometers for an 18-day cruise that took place in the North Atlantic during February 1996. The anemometers were distributed between the foremast platform, the main mast, and the bridge top (Fig. 1a). Two Young propeller vanes, one Windmaster sonic, and one Solent sonic were located on the foremast platform (Fig. 2).

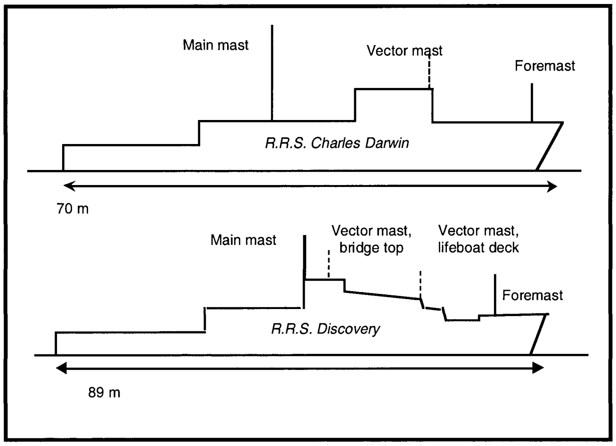

FIG. 1. Schematic of the anemometer sites on (top) the RRS *Charles Darwin* and (bottom) the RRS *Discovery*. The Vector mast (dashed lines) was not modeled.

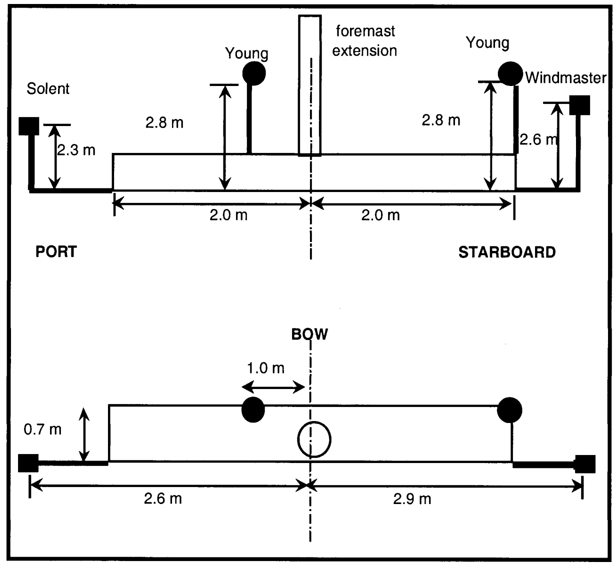

FIG. 2. Positions of the anemometers on the foremast platform of the RRS *Charles Darwin* looking from astern (top), and above (bottom).

The Solent sonic failed very early on in the cruise and did not provide any useful data. A second Young and a second Windmaster were located on top of the main mast, 2.0 and 1.0 m to port of the centerline of the ship, respectively. Five Vector anemometers were mounted on a temporary mast (a 7-m scaffold pole) located above the bridge (Fig. 3). The heights of the anemometers above sea level are listed in Table 1.

The RRS *Discovery* was equipped with nine anemometers for two 4-week cruises that took place in the North Atlantic (Leach and Pollard 1998) and in the Mediterranean (Allen and Guymer 1997) during November and December of 1996. The instruments were distributed between four sites (Fig. 1b). A Young propeller vane, a Windmaster sonic, and a Solent sonic were all mounted on the foremast platform (Fig. 4). A second Solent sonic was located on the top of the main mast. The foremast and main mast anemometers remained in the same positions for both *Discovery* cruises. The temporary 7-m mast equipped with five Vector anemometers was located at the front edge of the lifeboat deck during the first cruise and was then moved to the top of the bridge for the second cruise. The heights of the anemometers above sea level are listed in Table 1.

b. The in situ data

The 20-Hz output from the Solent sonic anemometers was logged for four 10-min periods every hour. Each sampling period was averaged to produce a 10-min mean relative wind speed value. Data from all the other anemometers were logged at 0.2 Hz, and were than averaged over the same 10-min periods.

The RRS *Discovery* results contained about 2700 ten-minute, averages, which were obtained for winds blowing within $\pm 30°$ of the bow. The maximum relative wind speed was 26 m s^{-1} and the mean was 14 m s^{-1}. The RRS *Charles Darwin* dataset contained about 500 ten-minute averages obtained for winds blowing within $\pm 30°$ of the bow. In this case the maximum wind speed was 17 m s^{-1} and the mean was 10 m s^{-1}. Although the *Darwin* cruises resulted in far fewer data, they are of particular interest since this ship presents a greater blockage to the flow to the foremast site (Fig. 5) and hence the anemometers experienced more significant flow distortion effects.

3. The CFD models

The commercially available finite volume CFD code ‘‘VECTIS’’ (Ricardo Consulting 2001) was used to calculate the three-dimensional, compressible, steady-state solutions of the time-averaged Navier–Stokes continuity and energy equations. The CFD solver is based on a Cartesian mesh and uses a bounded second-order hybrid differencing scheme to approximate the three momentum equations, and a first-order hybrid upwind differencing scheme for the pressure equation, the turbulent kinetic energy (k), and the rate of dissipation of turbulent kinetic energy (ε). Turbulence closure is obtained using a $k - \varepsilon$ turbulence parameterization with standard coefficients (Launder and Spalding 1974). It should be noted that the model results are used to investigate only the mean properties of the flow (mean speed and displacement). The turbulence properties of the CFD flow are not examined here.

Descriptions of the methods used to model the flow over the ships are given in detail in the references listed in Table 3 and will only be summarized here. To create a numerical model of a ship the 1:100 scale ‘‘general arrangement’’ plans were digitized and then converted into a three-dimensional geometry using the preproces-

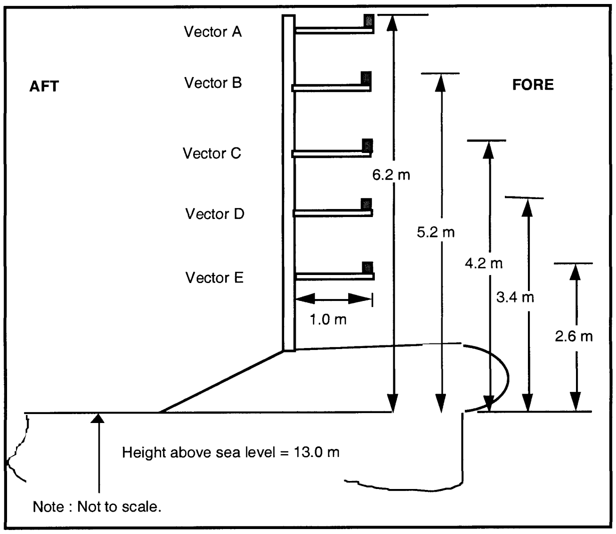

FIG. 3. Schematic side view of the Vector anemometers on the temporary 7-m mast above the bridge on the RRS *Charles Darwin.*

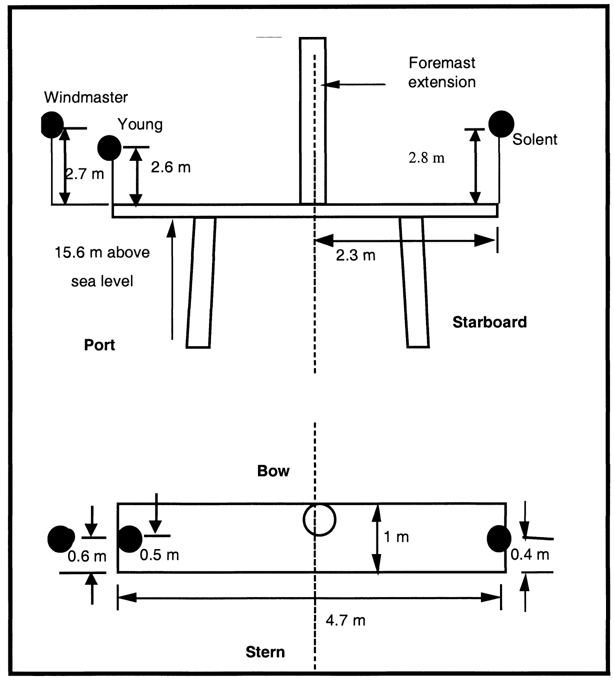

FIG. 4. The positions of the foremast anemometers on RRS *Discovery* cruises, viewed from astern (top) and above (bottom).

sor FEMGEN (Femsys Ltd. 1999), at which point the ship geometry was enclosed in a computational volume or "wind tunnel." The dimensions of the computational domain used for each ship were similar, with a wind tunnel length and height of 600 and 150 m, respectively. The width of the domain was chosen to ensure that the blockage of the flow in the tunnel by the ship was minimal (Castro and Robins 1977) and therefore depended on the angle of the ship to the flow. For the RRS *Charles Darwin* model the width was 300 m for a bow-on flow and 800 m for a flow at 30° to the bow. The geometry was then passed to VECTIS where the vertical profile of the velocity at the wind tunnel inlet was specified. For most models this profile was defined as logarithmic with a 10-m wind speed of 14 m s^{-1}. The domain floor was allocated a small roughness length (order 10^{-4} m) in order to maintain the profile downwind of the inlet. The number and the size of the computational cells within the domain were dependent on the processing power and memory size of the workstation used to solve the flow field. The models under discussion were limited to a total of about 250 000 cells. The size of the cells could be varied, allowing high resolution (cells of 0.2 m on a side) in the vicinity of the anemometer sites and much lower resolution in areas well away from the ship. Once the cell sizes were specified, the mesh was generated, and the model was run until the solution had converged; that is, the velocities at various monitoring locations were constant to within 0.1 m s^{-1}. The time taken for the solution to converge varied from two weeks using an SGI Origin 200 workstation to five weeks using an SGI Indigo^2. In order to check that the ship did not create a significant blockage to the flow in the tunnel, the speed of the flow at points well abeam of the ship was compared to the speed of the flow at the inlet and outlet. Since no significant blockage was found, the speed of the freestream flow was determined using a vertical profile of the wind speed at a point well abeam (more than 100 m) of the anemometer position.

Both the *Darwin* and the *Discovery* were modeled for a 14 m s^{-1} flow at five different relative wind directions: (i) 30° off the port bow, (ii) 15° off the port bow, (iii) bow-on, (iv) 15° off the starboard bow, and (v) 30° off the starboard bow. Figure 5 shows that the ships were reproduced in some detail in the model. However, it must be noted that smaller structures such as the rails around the platform and the instruments themselves were too small to be resolved in the model. In addition, any temporary installations would not be modeled.

The RRS *Charles Darwin,* the RRS *James Clark Ross,* and the RRS *Discovery* were all modeled at more than one wind speed and the results were used to investigate the dependence of the flow distortion on wind speed (section 6). Other research ships have been modeled in the same detail for bow-on flows at one wind speed only. These results are presented in section 7.

4. Comparison of the CFD and in situ wind speed results

a. Method

A direct comparison of the CFD model wind speeds with the in situ wind speed data was not possible since there was no in situ measurement of the undistorted, or freestream, flow. Instead, for each anemometer site a relative difference was obtained by dividing the wind speed measured by the anemometer with that from a

TABLE 1. The type, location, and height above sea level of the anemometers on the *Darwin* and the *Discovery*. The absolute wind speed error (% of freestream speed at the actual anemometer height, z_{anemom}) found from the CFD models are given for each site for five different relative wind directions. A wind direction of 0° indicates a bow-on flow, and a negative direction indicates a flow on to the port bow. A negative wind speed error indicates that the flow has been decelerated. The models used a freestream flow with a U_{10N} of 14 m s^{-1}.

Ship	Location	Anemometer	Height (m)	Absolute wind speed error (%) for relative wind directions				
				−30°	−15°	0°	15°	30°
Darwin	Foremast platform	Young (port)	15.7	−6.7	−6.5	−8.4	−6.6	1.1
		Young (stbd)	15.8	1.3	−4.1	−5.6	−5.1	−4.2
		Solent sonic	15.2	−2.9	−3.4	−4.0	−2.5	1.9
		Windmaster	15.5	1.9	−2.5	−3.8	−3.5	−3.1
	Main mast	Young AQ	24.7	3.2	2.9	2.9	3.3	3.7
		Windmaster	25.2	3.3	3.1	2.8	3.3	3.6
	Temporary mast on top of ridge	Vector A	19.2	6.4	5.6	4.2	6.0	7.2
		Vector B	18.2	7.9	7.1	−1.2	6.9	8.3
		Vector C	17.2	10.0	9.3	−7.1	7.8	8.1
		Vector D	16.4	12.6	11.9	−5.0	9.8	9.0
		Vector E	15.7	14.1	13.5	−1.6	11.6	9.7
Discovery	Foremast platform	Solent sonic	18.6	3.5	0.8	−0.8	−0.2	1.4
		Windmaster	18.5	0.8	−0.6	−1.0	0.8	3.6
		Young AQ	18.4	1.4	−0.2	−0.8	0.9	3.6
	Main mast	Solent sonic	25.2	4.9	3.7	3.0	3.3	3.7
	Temporary mast on lifeboat deck	Vector A	15.9	3.2	—	−7.5	−1.9	1.6
		Vector B	14.9	3.6	−4.6	−8.8	−2.5	1.7
		Vector C	13.9	3.9	−4.1	−14.7	−2.8	1.7
		Vector D	12.9	4.0	−4.5	−16.5	−3.5	1.8
		Vector E	11.9	3.5	−8.3	−16.1	−8.6	1.8
	Temporary mast on top of bridge	Vector A	20.2	7.8	1.6	−1.6	1.6	7.8
		Vector B	19.2	4.5	1.3	−4.3	1.3	4.5
		Vector C	18.2	4.5	1.3	−3.7	1.3	4.5
		Vector D	17.2	4.6	1.0	−7.1	1.0	4.6
		Vector E	16.2	3.5	−0.3	−8.2	−0.3	3.5

reference anemometer. A relatively well exposed anemometer on each ship was chosen as the reference: in the case of the *Darwin,* the Windmaster anemometer on the main mast was chosen, whereas for the *Discovery* the Solent anemometer on the foremast was used as the reference. Only measured wind speeds of 6 m s^{-1} and above were used in the analysis since below this speed the data were limited in number and rather noisy. Data were extracted from each of the CFD models at the various anemometer sites and model estimates of the relative differences were compared to those obtained from the in situ data.

It should be noted that the relative difference includes the effects of flow distortion at both anemometer sites and is therefore not a measure of the severity of the flow distortion at a particular site. The severity of the flow distortion is given by the absolute wind speed errors (determined from the CFD models), which are defined as the difference between the wind speed at a site and the freestream, or undistorted, speed at the same height, expressed as a percentage of the freestream speed. A second measure is the amount that the flow has been displaced vertically by the time it reaches the anemometer site (section 5), with the same displacement having a greater impact for instruments nearer the surface. The absolute wind speed errors are given in Table 1 and the vertical displacements are given in Table 2.

The data fall into two main groups, which will be discussed in turn below. Anemometers located on the relatively well exposed foremast and main mast sites experienced absolute wind speed errors of between −8% to +4%, and displacements of about 1.5 m (foremast) to 3 m (main mast): these data will be discussed first. The Vector anemometers, which were deliberately located in various badly exposed sites on the temporary mast, experienced flows that had been accelerated by between −16% to +14% and displaced by up to 6 m. These data will be discussed later.

b. The relative wind speed difference at well-exposed anemometer sites

Figure 6 compares the in situ and the model estimates of the relative differences for five different wind directions for the four well-exposed anemometers on the RRS *Charles Darwin.* The reference site used is that of the Windmaster on the main mast. The Young on the main mast was mounted close to the reference anemometer and experienced the same flow distortion, hence the relative difference is not significantly different from unity. The model and in situ results agree closely for this anemometer site. Close agreement is also found for the anemometer sites on the foremast platform, even for the port-side Young anemometer which was located only 1 m from the foremast extension and which experienced a flow which was decelerated by up to 8% (Table 1).

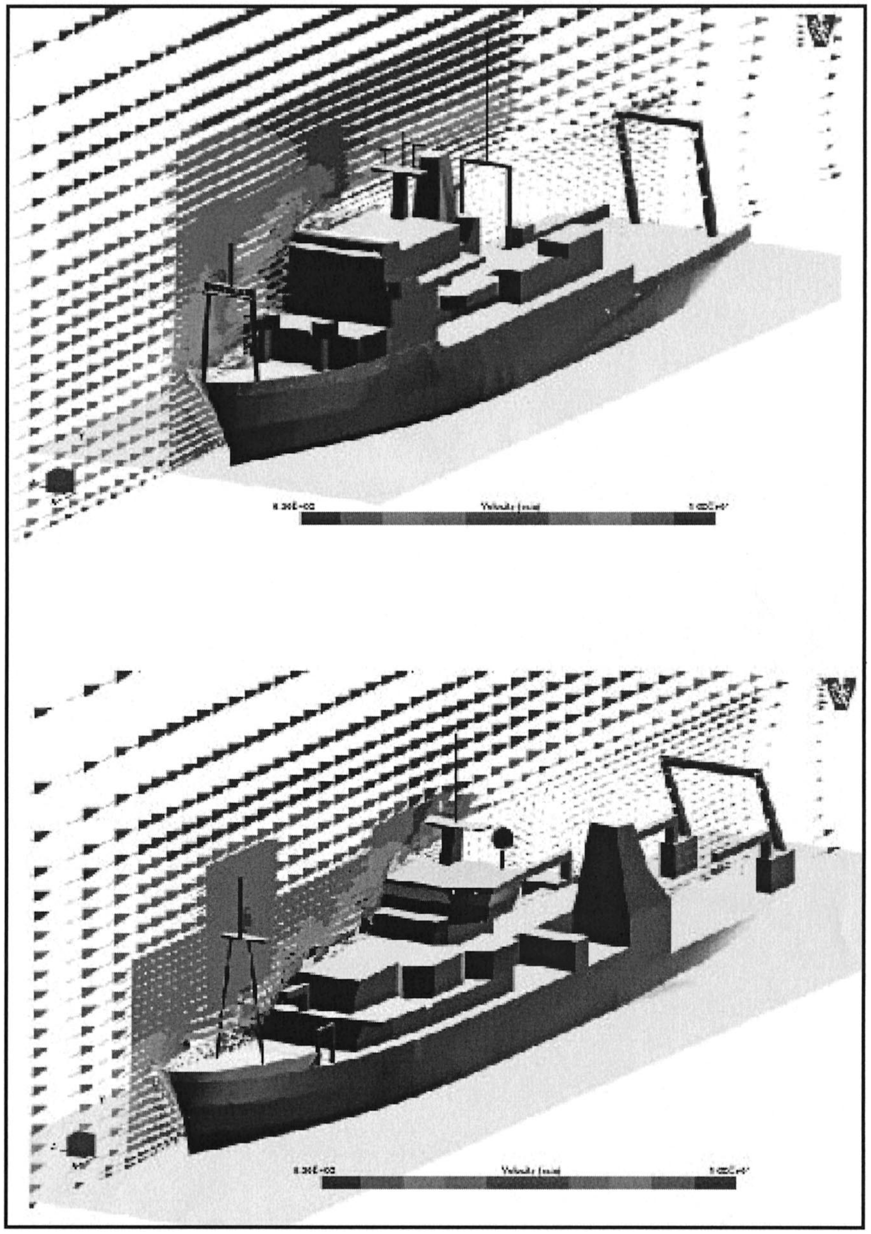

FIG. 5. The model representations of the *Darwin* (top) and the *Discovery* (bottom). The arrows represent the velocity of the flow in each computational cell, and the variable mesh density can be seen. In order to leave the ship geometry visible, only a two-dimensional slice of data is shown.

The least good comparison is found for the Windmaster sonic sited on the foremast where the model relative differences underestimate those from the in situ data by about 3% for all wind directions. However, given the specified instrument accuracies this comparison is still very good.

Figure 7 compares the in situ and the model estimates of the relative differences for the three well exposed anemometers on the RRS *Discovery.* The reference site is that of the Solent sonic on the starboard side of the foremast platform. Again the agreement is very good, especially for the main mast site. The agreement becomes less good for the two anemometer sites on the port side of the foremast platform when the wind is on the starboard bow. In these cases, the model underestimates the relative difference by between 3% and 6%. The results shown below (section 4c) for the Vector anemometer sites suggest that the model reproduces the flow at the reference anemometer site well for these wind directions, which in turn suggests that it is the flow to the sites on the port side of the platform which may be underestimated by the model for wind directions

TABLE 2. As in Table 1, but the absolute wind speed error is expressed as a percentage of the freestream speed at the *effective* anemometer height, $z_{anemom} - \Delta z$ (section 5a). The model estimate of the vertical displacement of the flow Δz is also given for each site.

				Absolute wind speed error (%) for relative wind directions					Vertical displacement of the flow (m)				
Ship	Location	Anemometer	Height (m)	−30°	−15°	0°	15°	30°	−30°	−15°	0°	15°	30°
Darwin	Foremast platform	Young (port)	15.7	−6.3	−6.0	−7.9	−5.8	2.1	1.5	1.4	1.2	1.4	1.4
		Young (stbd)	15.8	1.8	−3.6	−5.1	−4.4	−3.2	1.3	1.2	1.2	1.3	1.5
		Solent sonic	15.2	−2.1	−2.8	−3.4	−1.5	3.0	1.7	1.4	1.2	1.5	1.4
		Windmaster	15.5	2.5	−2.0	−3.3	−2.7	−1.9	1.4	1.2	1.2	1.3	1.6
	Main mast	Young AQ	24.7	4.3	3.7	3.3	4.3	5.2	3.7	2.6	2.2	2.5	3.7
		Windmaster	25.2	4.4	3.9	3.3	4.4	5.1	3.7	2.5	2.2	2.4	3.8
	Temporary mast on top of ridge	Vector A	19.2	7.7	6.6	5.3	7.4	10.3	3.3	2.8	2.9	2.8	3.2
		Vector B	18.2	9.5	8.3	2.0	8.5	11.1	3.6	3.1	3.1	3.0	3.4
		Vector C	17.2	11.9	10.8	−5.9	9.6	11.1	4.0	3.4	3.1	3.3	3.7
		Vector D	16.4	14.8	13.7	−3.7	12.1	12.3	4.4	3.7	3.0	4.1	3.9
		Vector E	15.7	16.7	15.8	1.8	14.4	13.1	4.7	4.2	6.2	4.6	4.1
Discovery	Foremast platform	Solent sonic	18.6	4.1	1.3	−0.4	0.3	2.1	1.5	1.2	1.1	1.4	1.8
		Windmaster	18.5	1.5	−0.1	−0.6	1.3	4.2	1.8	1.5	1.1	1.2	1.5
		Young AQ	18.4	2.2	0.3	−0.4	1.4	4.2	1.8	1.4	1.0	1.2	1.6
	Main mast	Solent sonic	25.2	6.1	4.6	3.8	4.2	4.9	3.7	2.7	2.3	2.9	3.6
	Temporary mast on life-boat deck	Vector A	15.9	4.6	—	−6.9	−0.8	3.2	2.9	—	1.6	2.5	3.3
		Vector B	14.9	5.0	−3.9	−8.1	−1.2	3.5	2.8	1.6	1.6	2.7	3.6
		Vector C	13.9	5.6	−3.3	−14.0	−1.3	3.6	3.1	1.7	1.6	3.0	3.9
		Vector D	12.9	6.0	−3.6	−15.8	−1.7	4.5	3.3	1.8	1.5	3.2	4.3
		Vector E	11.9	5.9	−7.4	−15.6	−6.5	5.4	3.6	1.8	1.4	3.6	4.8
	Temporary mast on top of bridge	Vector A	20.2	9.6	2.8	−0.7	2.8	9.6	4.4	3.2	2.5	3.2	4.4
		Vector B	19.2	6.5	2.7	−3.3	2.7	6.5	4.8	3.4	2.8	3.4	4.8
		Vector C	18.2	6.9	2.8	−2.7	2.8	6.9	5.3	3.7	2.8	3.7	5.3
		Vector D	17.2	7.4	2.9	−6.1	2.9	7.4	5.7	4.0	2.7	4.0	5.7
		Vector E	16.2	6.9	1.9	−6.9	1.9	6.9	6.3	4.5	3.1	4.5	6.3

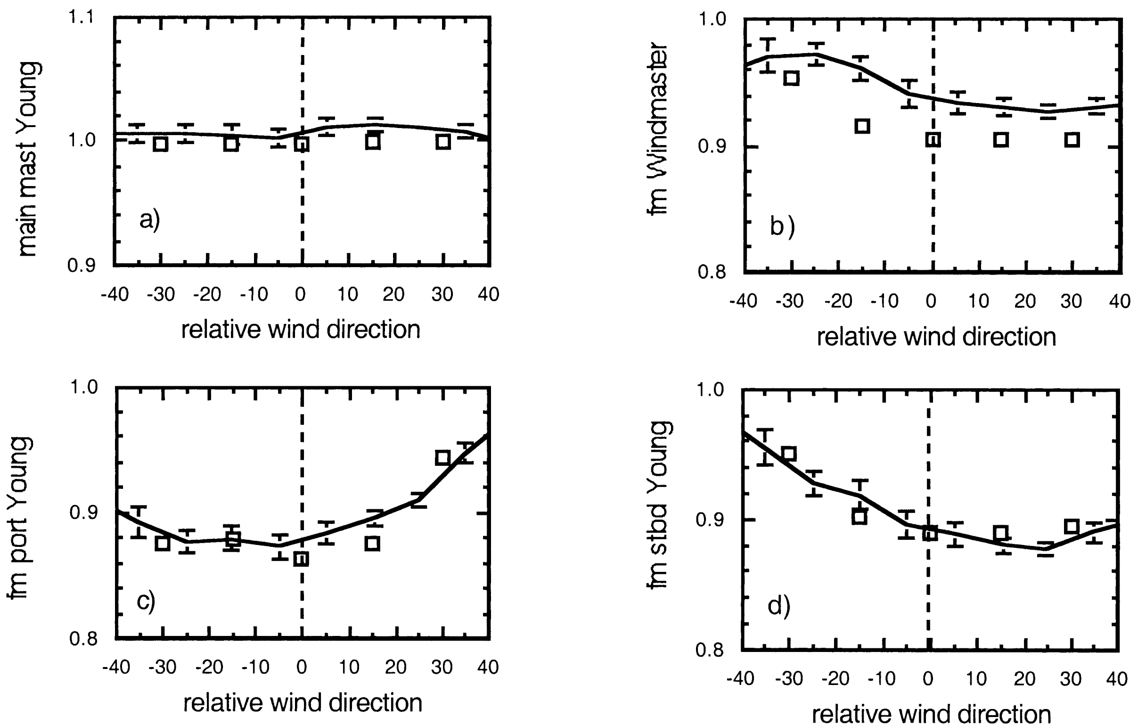

FIG. 6. Relative wind speed differences (expressed as a fraction of the wind speed measured by the Windmaster sonic on the main mast) from in situ wind speed measurements made on the RRS *Charles Darwin* (lines) and from the models (open squares) for different wind directions. Relative differences are shown for (a) the Young on the main mast, (b) the Windmaster sonic on the foremast, (c) the Young on the port side of the foremast platform, and (d) the Young on the starboard side of the foremast platform. The error bars indicate the standard error of the mean, and the dotted lines indicate bow-on flow (at 0°). Winds to port of the bow are shown by negative wind directions.

from the starboard side. A possible reason for this is the simplified way in which the foremast is represented in the model (Fig. 5); Fig. 8 shows that in reality the platform was rather cluttered.

These comparisons demonstrate that, in most cases, the CFD models of airflows within 30° of the bows of the ships are capable of reproducing the in situ estimates of the relative wind speed difference between pairs of anemometers to within 2%. This is a remarkably close agreement given the possible instrument errors. The slightly larger discrepancies found in a few cases could be due either to small biases in the in situ data (the Windmaster sonic on the *Darwin*) or due to the simplification of the foremast platform in the model (in the case of the port side anemometers on the *Discovery*).

c. The relative wind speed difference at anemometer sites with severe flow distortion

Figure 9 compares the in situ and the model estimates of the relative differences for the five Vector anemometers on the temporary mast located at the front edge of the bridge of the *Darwin.* The temporary mast was offset 1.7 m to port of the centerline of the ship, and was about 14 m aft of the foremast. The foremast extension (above the foremast platform) sheds a wake, the center of which coincides with the position of the temporary mast when the flow is 7° off the starboard bow. This angle is indicated in Fig. 9 by the dashed line, and the presence of the wake can be seen in both the in situ data and in the model simulations for the four lowest Vector anemometer sites. Within the wake region the model underestimates the relative differences by up to about 5%, which is reasonable agreement given that the CFD model is expected to reproduce such flows very badly.

Outside the wake region the model predictions agree closely with the data obtained from the Vector cup anemometer, with the model results tending to overestimate the relative differences by about 2% at most. The model results suggest that the mean flow at the anemometer sites was at an angle of 6° to 8° to the horizontal. If the Vector anemometers are assumed to have a cosine response, these angles suggest that up to 1% of the difference between the in situ and the model results can be attributed to the Vector anemometers slightly underestimating the flow. The only significant discrepancy between the models and the in situ data occurs at the site of the Vector ''A'' (highest) anemometer when the wind is on the port bow. In this case the models predict relative differences that are about 8% lower than those observed. However, the trend in the

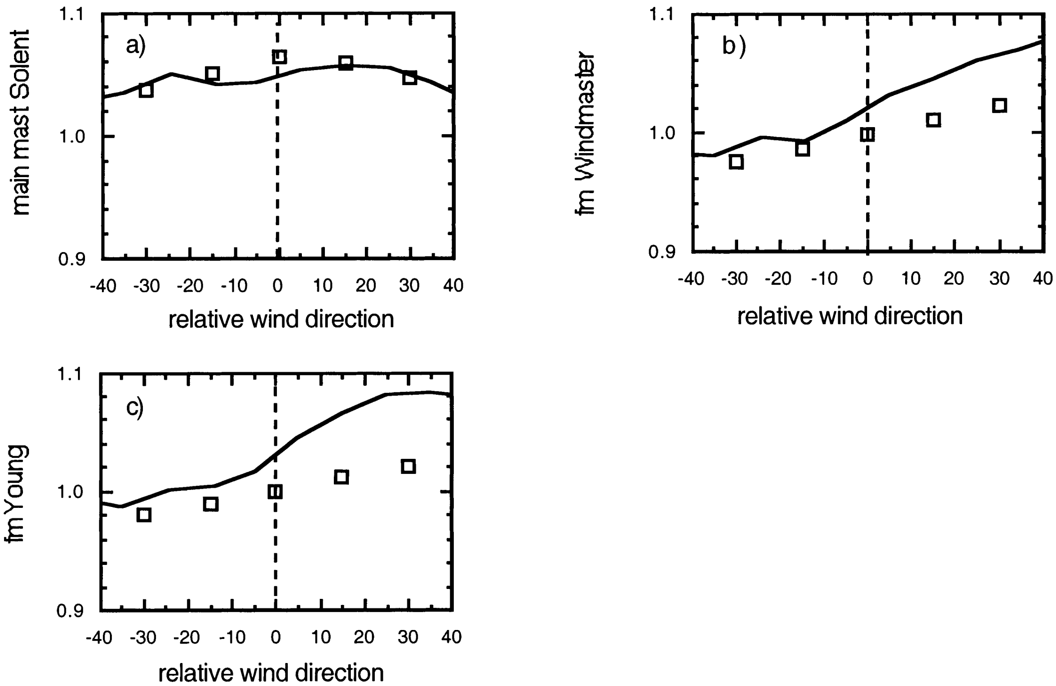

FIG. 7. Relative wind speed differences (expressed as a fraction of the wind speed measured by the Solent sonic on the foremast) from in situ wind speed measurements made on the RRS *Discovery* (lines) and from the models (open squares) for different wind directions. The standard errors ranged from 0.001 to 0.005 for the 10° averages of the in situ data. Relative differences are shown for (a) the Solent sonic on the main mast, (b) the Windmaster sonic on the foremast, and (c) the Young on the foremast. The dotted lines indicate bow-on flow (at 0°). Winds to port of the bow are shown by negative wind directions.

results from the lowest four anemometers of a decrease in the relative difference with height does not hold for Vector A, and unlike the data from the other four Vectors, the data from this instrument were not symmetrical with wind direction. Since there was no physical justification for such asymmetry (such as upwind obstacles), this suggests that the discrepancy is due to a problem with the in situ data, although the cause is unknown. The model estimates of the absolute wind speed errors at the Vector anemometer sites varied from accelerations of 14% to decelerations of 7%, an indication that the effects of flow distortion were severe. Despite this, the agreement between the model and the in situ data is excellent.

Figures 10 and 11 show the relative differences for the Vector anemometers mounted on the temporary mast located first on the lifeboat deck and then above the bridge of the *Discovery*, respectively. Again the wake of the foremast can be seen both in the model and in the in situ results. The mast was located on the centerline of the ship, hence the center of the wake intercepts the position of the temporary mast when the wind is bow-on, that is, for wind directions of 0°. When the Vectors were on the lifeboat deck, the wake was both broader and stronger than when they were moved to the top of the bridge. In the first case the anemometers were 11 m downwind of the mast and in a region that was affected by the wake cast by the two support legs of the foremast as well as the foremast platform itself. The in situ data from Vector ''E'' (the lowest on the mast) shows a wake that has a maximum for a flow at 10° to port rather than at a wind direction of 0° (Fig. 10e). It is thought that this instrument was affected by the presence of a large deck crane upwind. When the anemometers were moved to the top of the bridge they were 24.5 m downwind of the mast and were affected by the wake of the foremast extension only (Fig. 5). As expected, the model simulations of the flow in the center of the wake are poor, underestimating the relative difference by up to 15%.

In the case of the anemometers on the lifeboat deck (Fig. 10), the model and the in situ data agree to within 2% for flows more than 10° off the bow, that is, away from the strongest parts of the wake. The exception to this is the Vector E site, which is affected by the wake of the crane for all winds within 30° of the bow. In contrast, the comparison for the anemometer sites on top of the bridge (Fig. 11) suggests that the model consistently overestimates the relative differences outside the wake region by up to 5%. However, the angle of the flow to the horizontal varied from 7° to 14° and would result in the Vector anemometers underestimating the wind speed by between 1% and 3% assuming a cosine response. If this is taken into account, the model reproduces the in situ data to 3% or better, which is

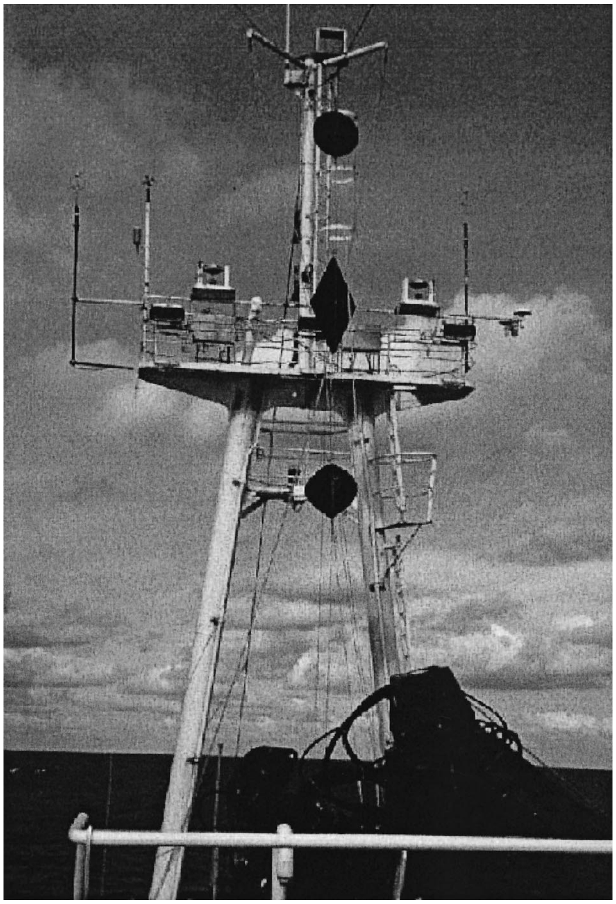

FIG. 8. The foremast platform of the RRS *Discovery,* viewed from astern.

again considered very good agreement for sites where the flow distortion is severe.

d. Conclusions

The results discussed above show that the detailed models of the two ships successfully reproduced the relative wind speed differences found from in situ data from pairs of anemometers. For the majority of anemometer sites the modeled relative differences agreed with the in situ data to within 2% or better, even for sites that experienced severe flow distortion. This agreement broke down under conditions where $k - \varepsilon$ CFD models are known to do badly (summarized in Versteeg and Malalasekera 1999), that is, where the anemometers were sited in the wake of the large foremast. Anemometers would not normally be located in such regions.

5. The vertical displacement of the flow

a. Method of validation

In addition to being accelerated (or decelerated), the flow of air over a ship may be displaced vertically due to the divergence of the flow around the ship. In the VECTIS CFD models it is possible to obtain streamline traces, which begin far upwind of the ship and pass near the anemometer site. The path of the streamline that intersects the anemometer site allows the vertical displacement of the flow reaching the site to be estimated. Such displacements have not been quantified in the field due to the practical problems involved, hence the model-derived estimates of the vertical displacement have to be verified indirectly. This section provides verification by comparing inertial dissipation measurements of the wind stress that were obtained from instrument sites that experienced a wide range of vertical displacements of the flow.

The inertial dissipation method obtains the dissipation rate of the turbulent kinetic energy ε using only the high frequency (>2 Hz) part of the wind speed spectrum. It is thought that this high frequency turbulence is not directly affected by flow distortion, unlike the lower frequencies that are required for stress measurement via the eddy correlation method (Edson et al. 1991; Oost et al. 1994). To correct eddy correlation estimates of the fluxes, it would be necessary to quantify the effects of flow distortion on these larger turbulent eddies explicitly; this cannot be done using the VECTIS code.

For neutral atmospheric stability the friction velocity u_* and the 10-m drag coefficient C_{D10N} are derived from the measurement of ε via the relationships (e.g., Taylor and Yelland 2000)

$$u_*^3 = kz\varepsilon \tag{1}$$

$$C_{D10N} = \frac{u_*^2}{U_{10N}^2}, \tag{2}$$

where k is the von Kármán constant, U_{10N} is the 10-m neutral wind speed, and z is the height at which the flow originated. In most studies, z is assumed to be the height of the anemometer, but the models results suggest that this is incorrect since the vertical displacement Δz of the flow to the anemometer is significant. As discussed in YT98, the time taken for a bow-on flow to be displaced from its original height to the height of the anemometer was small (less than 2 s) compared to the 5 s or more it would take for the turbulence to adjust to the new height (Henjes 1996). For this reason, YT98 employed the model results to allow for the vertical displacement by using

$$z = z_{anemom} - \Delta z, \tag{3}$$

where z_{anemom} is the height about sea level of the anemometer; that is, z becomes an ‘‘effective’’ anemometer height. YT98 showed that this, along with the application of the model-derived absolute wind speed errors, successfully reconciled the drag coefficient measurements made from five anemometers located on the foremasts of the *Darwin* and the *Discovery,* which had previously showed systematic biases of up to 60%. However, although the absolute wind speed errors used in

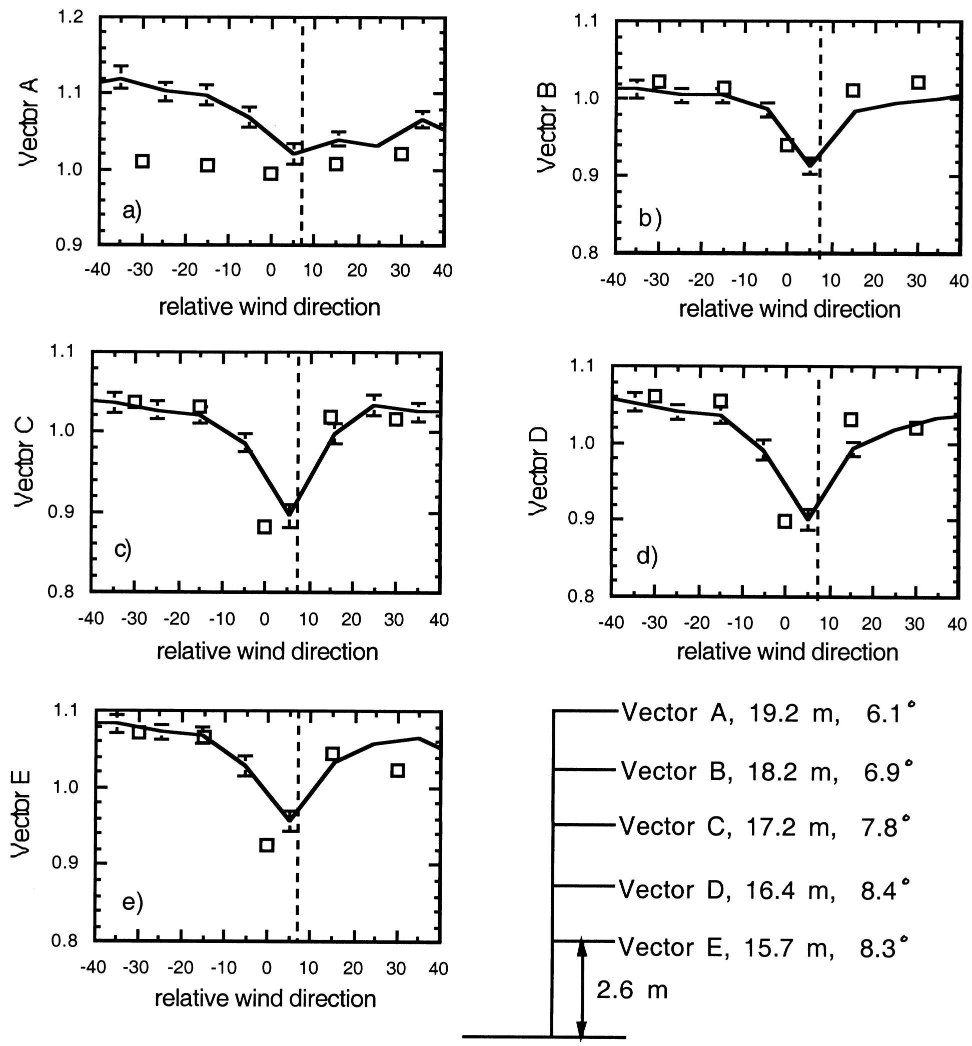

FIG. 9. The relative wind speed differences (expressed as a fraction of the wind speed measured by the Windmaster sonic on the main mast) from in situ wind speed measurements made on the RRS *Charles Darwin* (lines) and from the models (open squares) for the five Vector anemometers on the temporary mast above the bridge. The error bars indicate the standard error of the mean, and the dashed line indicates the center of the wake shed by the foremast. The schematic at the bottom right indicates the height above sea level of each anemometer and the angle of the flow to the horizontal (derived from the model results for a flow directly over the bow). The lowest anemometer was 2.6 m above the bridge top.

their study ranged from -13.5% to -0.5%, the values of Δz only varied from 1.0 to 1.2 m for the five anemometer sites. This meant that any significant error in the Δz estimate would affect the results from all the anemometers in a similar fashion. In other words, the Δz estimates used by YT98 were unvalidated.

It should be noted that the algorithm used in this study to calculate u_*, C_{D10N}, and U_{10N} assumes that the dissipation rate and the mean wind speed are both obtained from the same anemometer; that is, only one height is used. For this reason the wind speed corrections presented in Tables 2, 3, and 4 applies to the effective anemometer height, that is, the freestream wind speed used in calculating the correction is also obtained at the effective anemometer height. For typical displacements of the order of 1 m and anemometer heights of about 15 m, the impact of using the effective rather than the actual anemometer height on the wind speed error is less than 1% (Table 3).

In order to validate the model-derived estimates of Δz, it was necessary to obtain in situ wind stress data for flows that had been displaced through significantly different distances. Table 3 summarizes the effects of flow distortion at particular anemometer sites for bow-on flows over all the research ships that have been studied so far. Not all sites were occupied by fast sampling anemometers suitable for wind stress measurement. In addition, the authors only had access to the data from some of the fast sampling anemometers. Typically, research anemometers are located on a mast in the bows

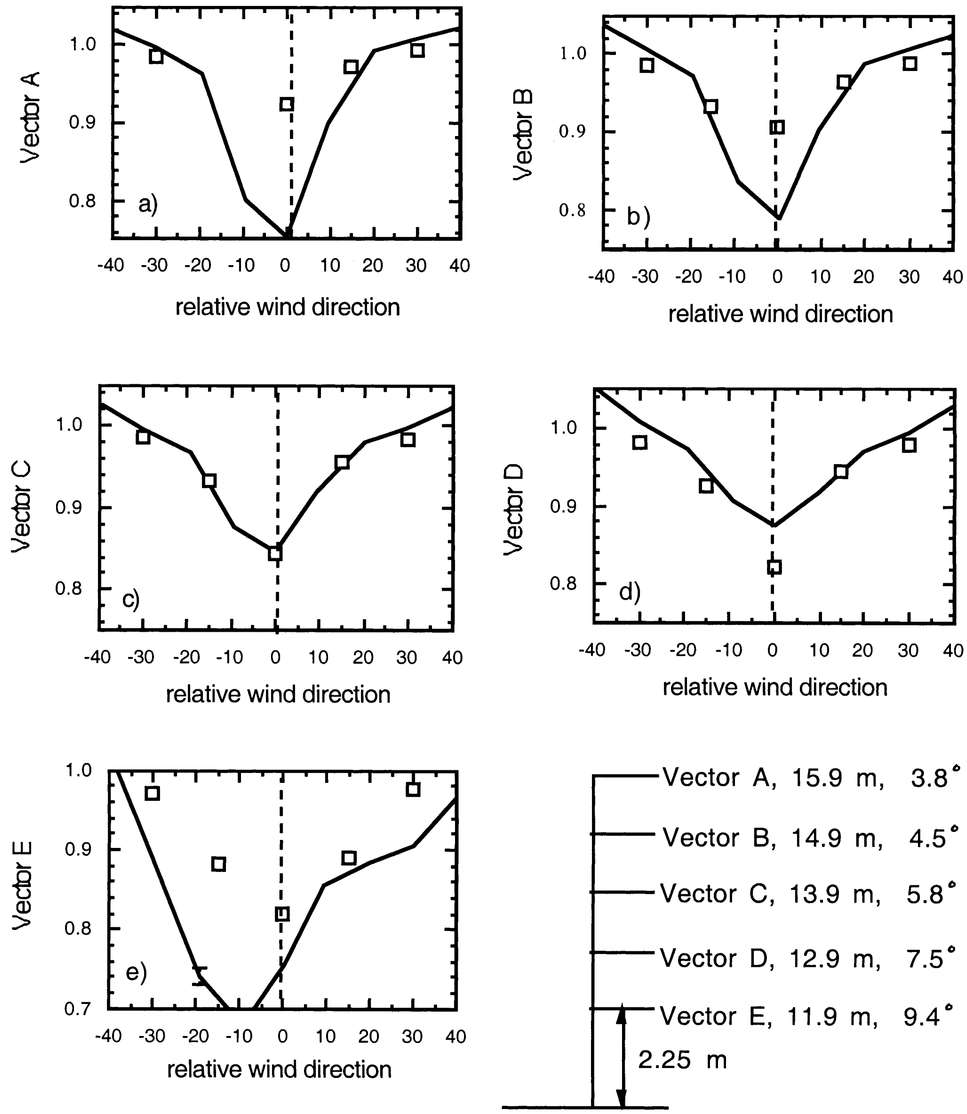

FIG. 10. The relative wind speed differences (expressed as a fraction of the wind speed measured by the Solent sonic on the foremast) from in situ wind speed measurements made on the RRS *Discovery* (lines) and from the models (open squares) for the five Vector anemometers on the temporary mast on the lifeboat deck in front of the bridge. The standard errors were typically between 0.002 and 0.007 for the 10° averages of the in situ data. The dashed line indicates the centre of the wake shed by the foremast. The schematic at the bottom right indicates the height above sea level of each anemometer and the angle of the flow to the horizontal (derived from the model results for a flow directly over the bow).

of the ship, at a height of between 15 and 20 m, and generally experience a flow that has been displaced vertically by about 1 m. Most of the ships have only been studied for bow-on flows. The exceptions to this are the *Darwin* and *Discovery,* which were modeled for flows at 0° (bow-on), 15°, and 30° off the bow (Tables 1 and 2), and the *James Clark Ross* and *Cumulus*, which were modeled for flows at 0° and −90° (a flow on to the port beam). The results for the latter two ships are given in Table 4 (schematics of the ships are shown in Fig. 16). The vertical displacement of the flow to the Solent sonic anemometers on the *Darwin* and *Discovery* only varied from 1.2 to 1.7 m and from 1.1 to 1.8 m (Table 2) as the direction of the flow changed from bow-on to 30° off the bow. In contrast, the vertical displacement of the flow to the anemometers on the OWS *Cumulus* and the *James Clark Ross* varied from about 1 to 4 m and from 1.6 to 5.2 m for bow-on and beam-on flows, respectively. Data from these two ships are used in the following sections to estimate the accuracy of the model-derived estimate of the vertical displacements. It should be noted that these ships were unusual in that they spent a significant amount of time beam-on to the wind: it is more usual that the majority of data are obtained while

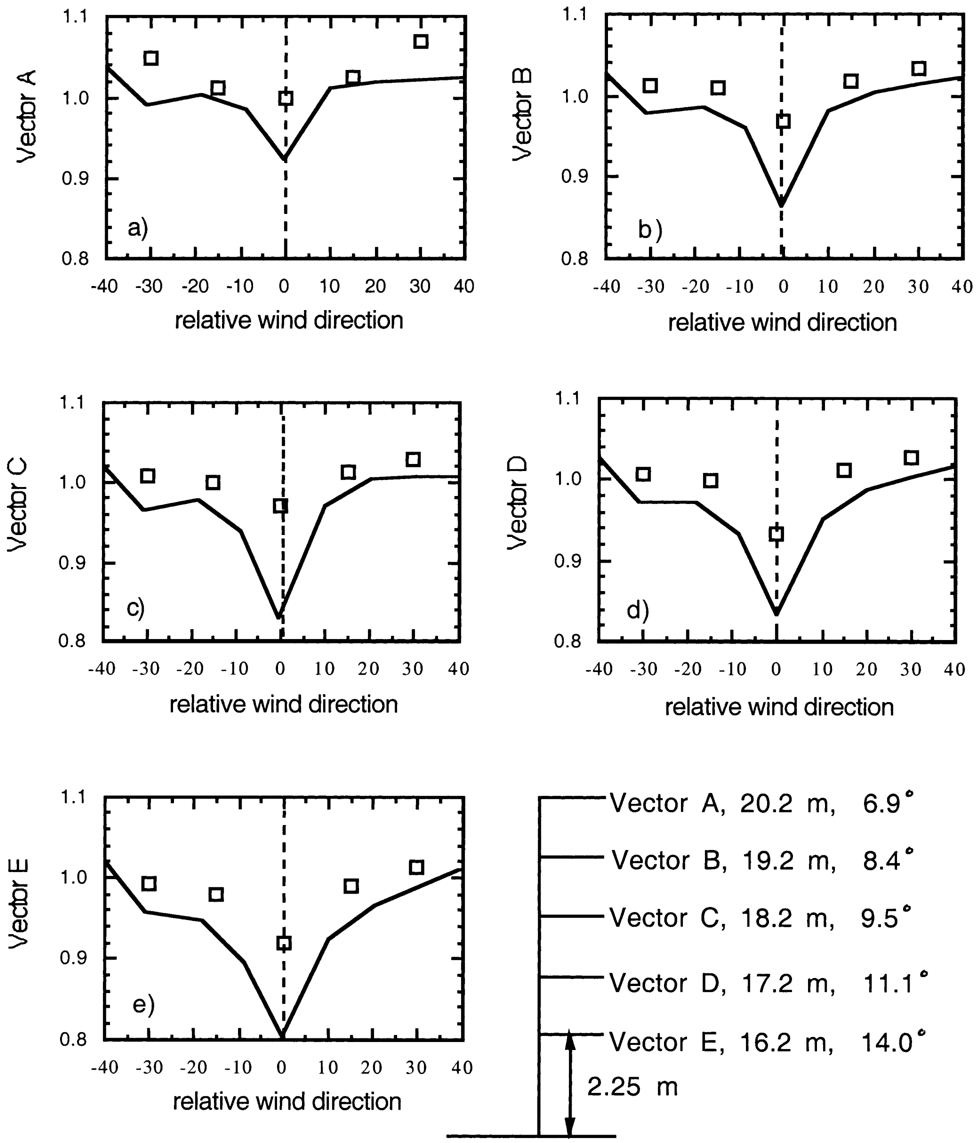

FIG. 11. The relative wind speed differences (expressed as a fraction of the wind speed measured by the Solent sonic on the foremast) from in situ wind speed measurements made on the RRS *Discovery* (lines) and from the models (open squares) for the five Vector anemometers on the temporary mast on top of the bridge. The standard errors ranged from 0.001 to 0.007 for the 10° averages of the in situ data. The dashed line indicates the centre of the wake shed by the foremast. The schematic at the bottom right indicates the height above sea level of each anemometer and the angle of the flow to the horizontal (derived from the model results for a flow directly over the bow).

the ship is bow-on to the wind, either while the ship is on-station or while steaming at speeds similar to or larger than the mean wind speed.

Since the previous section showed that the model estimates of the mean wind speeds were usually accurate to 2% or better, it will be assumed here that the modeled wind speed corrections are valid and that, once these have been applied to that data, any residual difference between the mean C_{D10N} to U_{10N} relationships is due to the vertical displacement of the flow.

b. RRS James Clark Ross

The RRS *James Clark Ross* was instrumented by the Southampton Oceanography Centre (SOC) for two 6-week cruises, one in the summer of 1999, which took place in the North Atlantic and the Greenland Sea (Bacon and Yelland 2000) and the other in the autumn of 2000, which took place between the United Kingdom and the Falkland Islands (Yelland and Pascal 2000). The usual mean meteorological instruments were deployed, as well as the HS Solent sonic anemometer. The wind

TABLE 3. Summary of results for all research ships modeled to date. In all cases the flow was directly on to the bow of the ship and the freestream U_{10N} was between 13 and 15 m s^{-1}. In the location column, ''fm'' denotes the foremast, ''fmp'' the foremast platform, and ''mm'' the main mast (usually above the accommodation block). The position of the masts are given in Fig. 17. Where a number of anemometers were mounted near to each other only the mean and range of the results are given. The acceleration of the flow has been calculated twice, once using the freestream speed at the actual anemometer height and once using the freestream speed at the effective anemometer height. The second column indicates the reference for each of the models, where ''B'' refers to Berry et al. (2001a,b,c), ''M'' refers to Moat et al. (2001), and ''MY'' refers to Moat and Yelland (1996a,b,c, 1997, 1998, 2001).

Ship (bow height, m)	Report	Instrument	Location	Anemometer height, z (m)	% accelerat^n ($z_{anemo} - \Delta z$)	% accelerat^n (z_{amenom})	Δz (m)
Challenger (4.5)	B2001C	Solent sonic	fm top	18.0	−0.9	−1.2	0.8
Cumulus (6.5)	MY1997	Solent sonic	fm	23.4	1.8	1.5	1.1
Darwin (6.0)	MY'96c	Solent sonic	fmp	15.2	−3.4	−4.0	1.2
		Windmaster	min	25.2	3.3	2.8	2.2
Dawson (5.9)	YT98	Gill propeller	Bowmast	12.4	−0.2	−0.6	0.4
		U2A	mm	18.7	5.5	4.8	1.1
Discovery (6.5)	MY'96b	Solent sonic	fmp	18.6	−0.4	−0.8	1.1
	MY2001	Solent sonic	mm	25.2	3.8	3.0	2.3
Hudson (7.0)	YT98	Unknown	Bowmast	15.4	−3.3	−4.1	1.1
		Unknown	mm	27.5	6.0	5.0	2.4
		Various	Lattice mast	17.3 ± 0.2	−2.0 ± 0.1	−2.7 ± 0.1	1.1
James Clark	B2001b	Ship's sonic	fm top	21.5	−1.1	−1.6	1.5
Ross (7.1)		Solent sonic	fmp	15.9	−0.4	−1.3	1.6
Knorr (6.7)	MY1998	Various	Lattice mast	18.4 ± 0.2	−0.8 ± 0.1	−1.1 ± 0.1	0.7
		Young	fm	19.2	1.0	0.4	1.3
		Various	Bowmast	15.5 ± 0.3	−2.2 ± 0.1	−2.4	0.4
Polarstern (9.4)	B2001 a	Sonic 5	Lattice mast up-	20.0	−6.0	−6.3	0.7
		Sonic 4	wind of bow	13.0	−10.5	−10.7	0.4
		Sonic 3		8.0	−12.7	−13.0	0.2
		Sonic 2		5.4	−13.9	−14.1	0.2
		Sonic 1		3.8	−15.2	−15.5	0.2
Ron Brown (6.4)	M2001	Two IMET	Lattice	14.4	−3.5 ± 0.1	−3.9 ± 0.2	0.7
		Sonic	Jackstaff	17.9	−3.7	−4.0	0.7
Suroit (5.7)	MY'96a	Solent sonic	10-m mast	16.1	−0.3	−0.7	0.8

stress was calculated as described in Taylor and Yelland (2000). On both cruises the Solent sonic anemometer was sited on the foremast platform 1.4 m to port of the ship's centerline and at a height of 15.85 ± 0.1 m above sea level. Although care was taken to mount the anemometer with the support strut facing aft, comparison with the ship's sonic anemometer suggested that the Solent was misaligned by about 2° on the first cruise and 6° on the second. The alignment of the ship's anemometer was used to provide a reference wind direction since this instrument is permanently installed and its alignment is unchanged from one cruise to the next. Examination of the model of the flow around the ship indicated that beam-on flows to the anemometer were deflected slightly forward around the accommodation block and would appear to come from 7° aft of the beam. The data from both cruises were corrected for the misalignment of the anemometer and for the 7° deflection for beam-on flows prior to analysis. The cruises were initially analyzed separately, but since the results were identical, the two datasets were subsequently merged and are presented here without differentiation.

The model of a bow-on flow over the ship showed that the flow reaching the anemometer had been decelerated by 0.4% and displaced vertically by 1.6 m. For beam-on conditions, the flow to the anemometer was accelerated by 13% and displaced by 5.2 m. Data were selected for corrected relative wind directions of −5° to 5° and −95° to −85° for bow-on and beam-on flows, respectively. Figure 12 shows the difference between

TABLE 4. The effect of flow distortion at the two anemometer sites on the OWS *Cumulus* and at the single anemometer site on the RRS *James Clark Ross* for bow-on and beam-on flows. The anemometer site on the goalpost mast on the *Cumulus* was affected by the wake of the foremast for bow-on flows. The models used a freestream flow with a U_{10N} of 14 m s^{-1}.

Ship	Anemometer location	Anemometer height (m)	Ship's orientation to the flow	Percent acceleration ($z_{anemon} - \Delta z$)	Δz (m)
OWS *Cumulus*	Foremast	23.4	Bow-on	1.8	1.1
	Foremast		Beam-on	4.9	4.0
	Goalpost	24.0	Beam-on	1.7	4.4
RRS *James*	Foremast		Bow-on	−0.4	1.6
Clark Ross	Platform	15.9	Beam-on	13.0	5.2

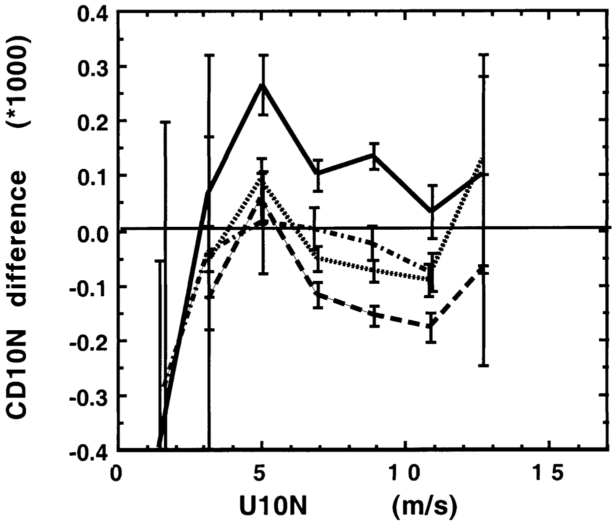

FIG. 12. The difference between the beam-on and bow-on C_{D10N} data obtained from the *James Clark Ross* cruises. The error bars indicate the standard error of the mean. Data are shown with wind speed corrections only, (solid line), with corrections for both the wind speed and the full Δz estimates (dashed line), with the wind speed correction and the last 2 s of Δz (dotted), and with wind speed corrections and the full Δz estimate assuming a 10° offset (chain).

the mean C_{D10N} data obtained for beam-on flows and that obtained for bow-on flows (i) if the wind speed correction only is applied (solid line) and (ii) if both the wind speed corrections and model Δz estimates are applied (dashed line). When only the wind speed correction is applied, there is a systematic difference between the beam-on and bow-on C_{D10N}, with the beam-on results being about 0.1×10^{-3} larger than the bow-on values for all bar the lowest wind speeds. Application of the Δz correction reverses this result to some extent, with the beam-on C_{D10N} results being smaller than the bow-on for winds between 7 and 12 m s^{-1}.

This result suggested that either 1) the Δz estimate is too large, especially for the beam-on flow, or 2) the assumption that the turbulence has not adjusted to the displacement is not valid. Figure 13 shows the variation of the vertical displacement with distance upstream of the anemometer position for both bow-on and beam-on flows. Since both models used a 10-m freestream speed of about 14 m s^{-1}, it can be seen that, for the bow-on flow almost all of the 1.6-m displacement took place in the last 2 s prior to the flow reaching the anemometer site. In contrast, for the beam-on model the displacement of the flow began about 7 s (100 m) upstream, and only 4 m of the total displacement (of 5.2 m) took place in the last 2 s. This suggests that the turbulence may have adjusted, at least partly, to its new height by the time it reaches the anemometer. Since the turbulence adjustment time is thought to be of the order of 5 s or more (Henjes 1996), it was thought reasonable to ignore the displacement that took place in the first 5 s, that is, to assume that the turbulence had adjusted to the all bar the last 2 s of the displacement. This was done by applying a Δz correction of 4.0 m for the beam-on flow and 1.5 m for the bow-on flow and resulted in a good agreement between the two (Fig. 12, dotted line).

An alternative explanation lies in a possible systematic error in the relative wind direction. The chain line in Fig. 12 shows the effect on C_{D10N} if a 10° offset is assumed in the relative wind direction. In this case both the wind speed correction and the full (5.2 m) vertical

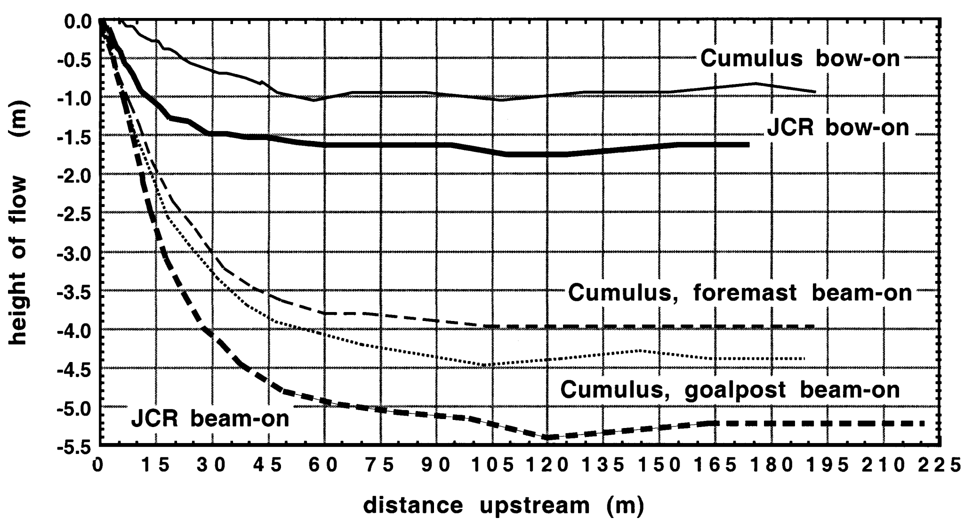

FIG. 13. The variation of the vertical displacement of the flow with distance upwind of the anemometer. The anemometer coordinates are at $x = 0$, $y = 0$. The data from the *James Clark Ross* model with a bow-on flow are given by the thick solid line and those for a beam-on flow by the thick dashed line. Bow-on flow to the foremast site on the *Cumulus* is shown by the thin solid line and beam-on flows to the foremast and goalpost sites are shown by the thin dashed and thin dotted lines, respectively. The freestream U_{10N} was 14 m s^{-1} in all cases.

displacement correction have been applied. It can be seen that this also brings the beam-on and bow-on C_{D10N} results into good agreement. This result also highlights the sensitivity of the flow distortion to the relative wind direction.

c. *OWS* Cumulus

For some years, the Institute of Oceanographic Sciences (now transferred to SOC) instrumented the OWS *Cumulus* with the mean meteorological system ''MultiMet'' (Birch and Pascal 1987) and a Solent sonic anemometer. The weather ship *Cumulus* occupied station LIMA (57°N, 20°W) in the North Atlantic for 4 weeks in every five, until the ship was decommissioned in June 1996. The *Cumulus* operated in two modes: 1) during low and moderate wind speed conditions the ship drifted beam-on, with the wind blowing onto the port side; and 2) in high winds speeds and/or large seas the ship ''hove-to'' and steamed slowly into the weather. The anemometer was initially situated on the port side of the ship's ''goalpost'' (middle) mast until this mast was removed in April 1993. After this date, the anemometer was situated on the ship's foremast until the IOS instrumentation was removed in June 1994.

IOS staff serviced the instruments and collected data between cruises but did not sail on the *Cumulus.* For this reason, many of the 4-week cruises did not result in complete datasets due to the failure of a logging system or a particular sensor, and the data quality was generally rather poor. In particular, the orientation of the anemometer was not properly recorded and the quality control criterion of selecting data where the true wind direction from the anemometer was within 10° of that reported in the ship's meteorological observations does not eliminate anemometer misalignments. However, the anemometers on the *Cumulus* were located much farther from the ship's superstructure than the anemometer on the *James Clark Ross* (Fig. 16), and the flow distortion at the former sites was thus less sensitive to changes in the relative wind direction.

While the anemometer was on the goalpost mast, complete datasets were obtained from four cruises (numbers 65, 70, 73, and 76) between April 1992 and May 1993. While the anemometer was on the foremast, complete datasets were obtained from three cruises (numbers 78, 79, and 80) between July and October 1993. The anemometer site on the goalpost mast was affected by the wake of the foremast for bow-on flows. For this reason only beam-on flows will be considered from this site.

The *Cumulus* was modeled for a flow directly over the bows and also for a flow onto the port beam (Table 4). It can be seen that for a bow-on flow, the anemometer on the foremast experienced relatively little flow distortion, with the flow being accelerated by less than 2% and displaced vertically by just over 1 m. However, as may be expected, the vertical displacement of the flow

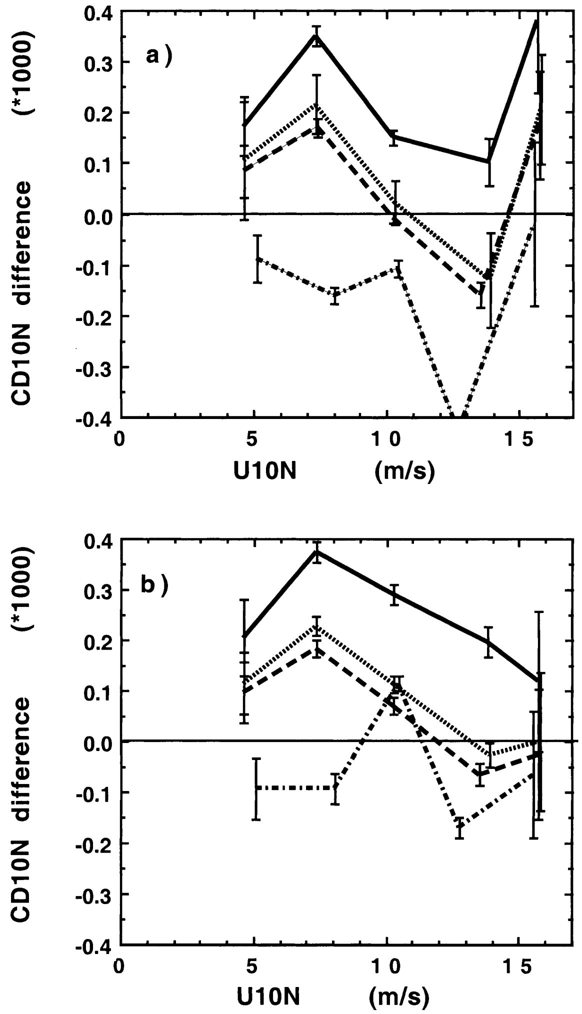

FIG. 14. The OWS *Cumulus* (beam − bow) C_{D10N} differences using (a) foremast beam-on flows minus foremast bow-on flows, and (b) goalpost beam-on flows minus foremast bow-on flows. The error bars indicate the standard error of the mean. Data are shown with wind speed corrections only (solid line), with corrections for both the wind speed and the full Δz estimates (dashed line), with the wind speed correction and the last 2 s of Δz (dotted), and with wind speed corrections and the full Δz estimate assuming a 10° offset (chain).

is much greater for a beam-on flow, with the anemometer sites on the foremast and the goalpost mast experiencing flows that have been displaced by 4.0 and 4.4 m, respectively. Data from the cruises above were selected for bow-on (±5°) and beam-on (±5°) flows, and were processed using (i) the mean wind speed corrections only and (ii) applying both corrections as listed in Table 4. The mean differences between the C_{D10N} results from beam-on and bow-on flows to the foremast site are shown in Fig. 14a, and those from beam-on flows to the goalpost site and bow-on flows to the foremast site are shown in Fig. 14b.

When the mean wind speed only is corrected by the amounts suggested by the model results, the beam-on flows both result in C_{D10N} values that are larger than those obtained for bow-on flows by about 0.2×10^{-3} to 0.3×10^{-3} for all wind speeds. Application of the full Δz estimate from the models brings the beam-on and bow-on data into reasonably good agreement.

This result contradicts that found from the *James Clark Ross* in that the full Δz estimate was required to bring the *Cumulus* bow- and beam-on data into agreement, whereas the full Δz may have overcorrected the results from the *James Clark Ross.* The vertical displacement of the flow to the anemometer sites on both ships show similar behavior (Fig. 13) in that the displacement begins about 7 s upstream for the beam-on models. However, the displacement of the bow-on flow over the *Cumulus* also begins 7 s upstream, whereas that for the *James Clark Ross* began just over 2 s upstream. If only the last 2 s of displacement are used as the height correction, then the Δz estimate for the *Cumulus* bow-on case becomes 0.7 m and for beam-on becomes 3.0 or 3.3 m for the foremast and goalpost mast sites, respectively. Since 1) the bow-on Δz estimate has also been reduced, and 2) the change in Δz estimate is small compared to the anemometer height (24 m for the *Cumulus* compared to 16 m for the *James Clark Ross*), the impact of using the 2 s rather than the full Δz estimate on the difference between bow- and beam-on data is much smaller in the case of the *Cumulus.*

d. Discussion

The previous sections attempted to validate the model-derived estimates of Δz, the vertical displacement of the flow reaching the anemometer sites. Since the validation of the mean wind correction showed that the modeled mean wind speed errors were accurate to within a couple of percent (section 4), it has been assumed here that the modeled wind speed errors are correct and that, once these have been applied to the data, any residual difference in the mean C_{D10N} to U_{10N} results is due to the vertical displacement of the flow. The *Cumulus* and the *James Clark Ross* were chosen since these ships had been modeled for both bow-on and beam-on flows and in situ wind stress data were available from both. In both cases the models suggested small (1–1.6 m) Δz values for bow-on flows and large (4–5.2 m) Δz values for beam-on flows. In the case of the *Cumulus* it was seen that the application of the full Δz estimates produced good agreement in the mean C_{D10N} results, but in the case of the *James Clark Ross* the C_{D10N} to U_{10N} results suggested that the Δz estimate was too large, and that a value of 4.0 m would produce much better agreement than the model estimate of 5.2 m. One explanation for this could be that the displacement of the flow for the beam-on case begins much farther upstream, and that the turbulence has adjusted to all but the final 2 s of the displacement. In contrast, the displacement of the flow to the *Cumulus* anemometer sites showed similar behavior (Fig. 13), but in this case the full Δz estimate results in good agreement. However, since the bow-on vertical displacement for the *Cumulus* also began more than 2 s upstream, using only the 2-s estimate of the displacement also produced a reasonable agreement between the bow- and beam-on cases. It is therefore not possible to show whether the turbulence does indeed adjust to the first 5 s of the displacement or whether the apparent overcorrection to the *James Clark Ross* results, which is produced by the application of the full Δz estimate, is due to a bias in the relative wind direction.

In summary, the validation of the model estimate of the vertical displacement of the flow is not completely conclusive in that it has not been possible to show whether the full Δz estimate should be used, or whether only the final 2 s of displacement should be used. However, it should be noted that the uncertainty in the appropriate value is usually insignificant for bow-on flows, and is only about 25% (1 m) for beam-on flows. In addition, it has been shown that the application of one or other of the Δz estimate greatly improves the beam-on results when compared to those obtained with the wind on the bow. Most data are obtained when the relative wind direction is on the bow, since the ships are either head-to-wind while on station or are steaming at speeds similar to or larger than the mean wind speed. For bow-on flows the Δz estimate is usually of the order of 1 m, and for most research ships modeled this displacement takes place in less than 2 s. It is therefore thought that the results show that the Δz estimate for bow-on flows is valid, but that some care should be taken when choosing the Δz value to apply for beam-on flows or in other situations where the vertical displacement is very large and begins a significant distance upstream of the anemometer.

6. Variation of the flow distortion with wind speed

This section considers the behavior of the flow distortion with relative wind speed. The RRS *Charles Darwin* was modeled for bow-on flows with a U_{10N} of 8 and 14 m s^{-1}, the RRS *Discovery* for bow-on flows with a U_{10N} of 6, 14, and 20 m s^{-1}, and the *James Clark Ross* for flows of 5 and 15 m s^{-1}. Data from the cruises discussed in the previous sections were used to examine the wind speed dependence of the relative differences in the wind speed measurements from pairs of anemometers. Data were selected for flows within $\pm 5°$ of the ships' bows. Two widely separated anemometer sites were selected from each ship, since adjacent anemometers experience similar flow distortion. Data from the sonic anemometers were chosen in preference to the Young propeller anemometers, since the latter perform less well at the lower wind speeds. Data from the Vector anemometers were not used since these instruments were in the wake of the foremast for bow-on flows. Figure 15 shows the relative wind speed differences from 1) the Solent anemometer on the foremast top normalized by the Solent HS anemometer on the fore-

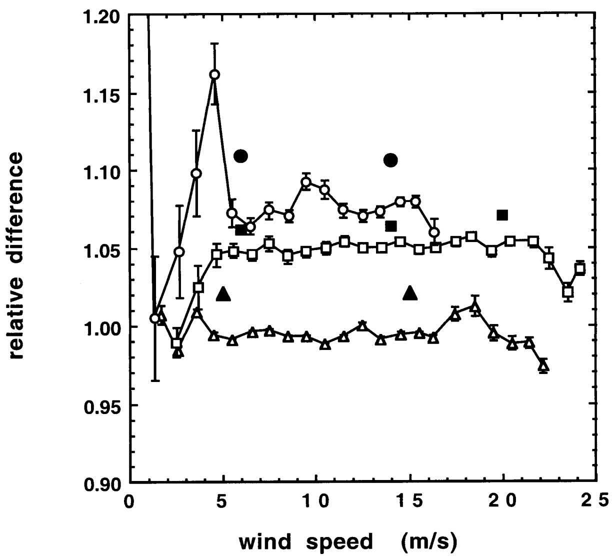

FIG. 15. Relative wind speed differences from pairs of anemometers. In situ data from the *Darwin* (○), the *Discovery* (□), and the *James Clark Ross* (△) are shown by the lines with open symbols and the error bars indicate the standard error of the mean. The solid symbols show the results from the models at various wind speeds. The relative differences were obtained by comparison of the mainmast anemometer data with the foremast anemometer data in the case of the *Darwin* and the *Discovery*, and by comparison of the data from the anemometer on the top of the foremast extension with those from the foremast platform in the case of the *James Clark Ross.*

mast platform of the *James Clark Ross*, 2) the Solent on the mainmast normalized by the Solent on the foremast platform of the *Discovery*, and 3) the Windmaster sonic on the mainmast normalized by the Windmaster on the foremast platform of the *Darwin.* Also shown are the results from the various models. Table 5 gives the model-derived absolute wind speed errors and the vertical displacement of the flow for the various anemometer sites.

It can be seen that the model-derived relative differences (Fig. 15) and the model-derived absolute wind speed errors (Table 5) both show very little variation with wind speed, with a maximum variation in the relative difference of less than 1% for the *Discovery* models at 6 and 20 m s^{-1}. DGH similarly found little or no dependence of their modeled wind speed correction with incident wind speed. Although the model results overestimate the relative differences for the *Discovery* and the *James Clark Ross* by 1% or 2%, the lack of variation with wind speed is confirmed by the in situ data. The overestimate of the model results is larger for the less-accurate Windmaster on the *Darwin*, but these data also suggest that there is no significant variation of the relative difference with wind speed.

Although the absolute wind speed errors vary little with wind speed, the models suggest that the vertical displacement Δz of the flow may decrease with increasing wind speed. The vertical displacement of the flow in the *Discovery* models varied from 1.3 to 0.7 m at the foremast site and from 2.6 to 1.8 m at the main mast site as the wind speed increased from 6 to 20 m s^{-1}. Use of a constant 1.0-m value for Δz for data obtained at the foremast site on the *Discovery* would introduce relatively small errors in the C_{D10N} to U_{10N} results for all wind speeds below 20 m s^{-1} (section 8).

7. Other research ships

The airflow over a number of research ships have been modeled during recent years. The CFD-derived estimates of the absolute wind speed error and the vertical displacement of the flow for each ship are presented in Table 3, along with the particular instrument locations examined. In all cases, the models used a bow-on flow with a U_{10N} of between 13 and 15 m s^{-1}. Two-dimensional schematics of the ships are shown in Fig. 16. Figure 17 shows the absolute wind speed error and the vertical displacement for all the anemometer sites in Table 3 against the distance of the anemometer downwind of the ship's bow.

Anemometers mounted above the superstructure on

TABLE 5. The effects of flow distortion from models with different freestream U_{10N} values. All models were of bow-on flows.

Ship	Location	Anemometer	Height (m)	Model U_{10N} (m s^{-1})	Percent acceleration (z_{anemom})	Δz (m)
Charles Darwin	fm platform	Windmaster	15.5	8	−3.5	1.3
	mainmast	Windmaster	25.2	8	2.6	2.3
	fm platform	Windmaster	15.5	14	−3.8	1.2
	mainmast	Windmaster	25.2	14	2.8	2.2
Discovery	fm platform	Solent	18.6	6	−0.9	1.3
	main mast	Solent	25.2	6	2.7	2.6
	fm platform	Solent	18.6	14	−0.8	1.1
	main mast	Solent	25.2	14	3.0	2.3
	fm platform	Solent	18.6	20	−1.1	0.7
	main mast	Solent	25.2	20	3.1	1.8
James Clark Ross	fm platform	Solent	15.9	5	−1.8	1.9
	foremast top	Ship's Solent	21.5	5	−1.7	1.7
	fm platform	Solent	15.9	15	−1.3	1.6
	foremast top	Ship's Solent	21.5	15	−1.6	1.5

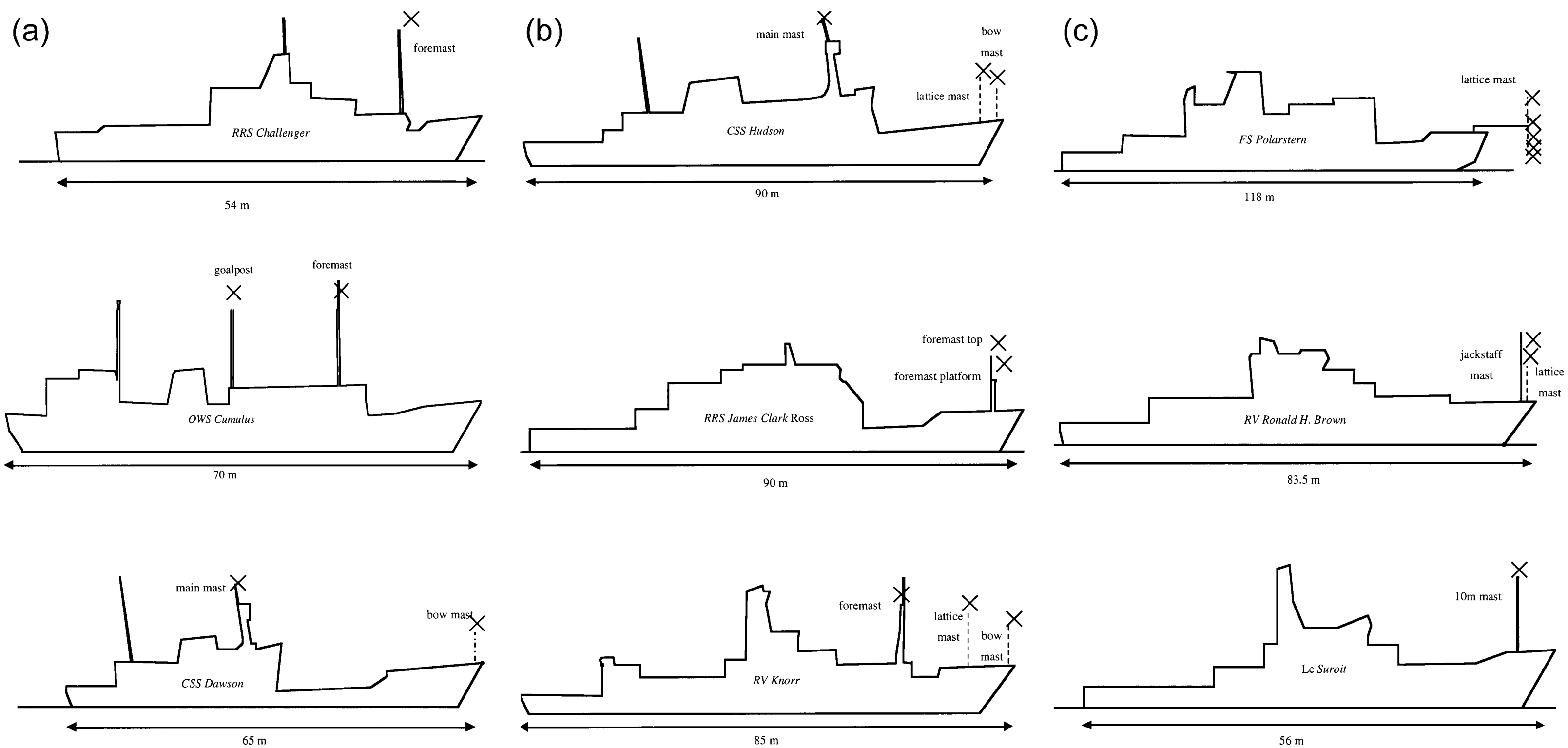

FIG. 16. Schematic representations of the various research ship models. Masts that were not included in the model geometry are indicated by the dashed lines. Not all masts are located on the centerline of the ship. Approximate anemometer sites are indicated by X.

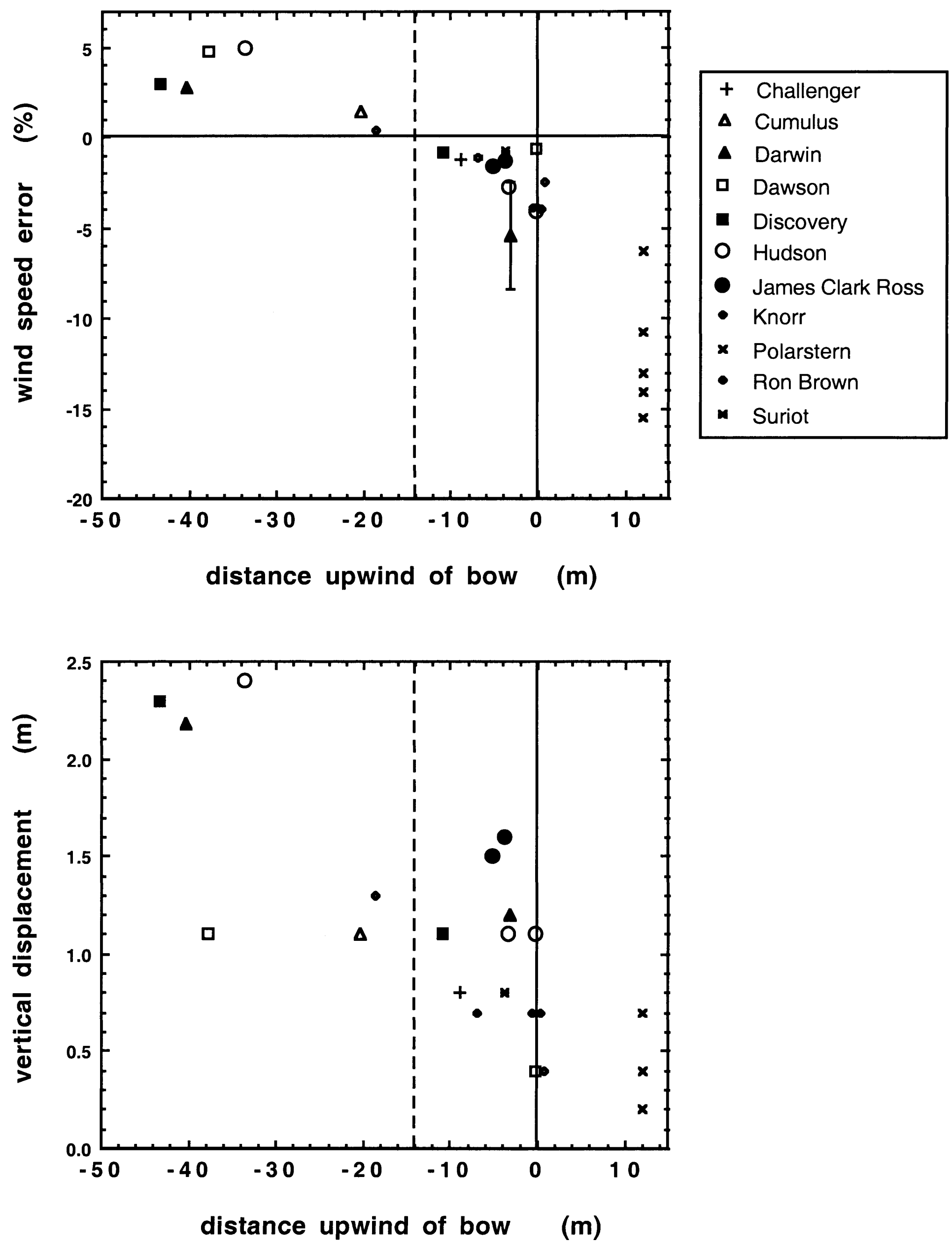

FIG. 17. The absolute wind speed error (top) and the vertical displacement of the flow (bottom) for the anemometer sites in Table 3. The *x* axis gives the position of the anemometer relative to the tip of the bow. The dashed line separates those anemometers mounted in the bows (to the right) from those mounted above the superstructure farther aft (left). Where multiple anemometers were located close together on a particular mast only the mean result is given, with an error bar to indicate the range of results found.

the ships' main masts tended to experience flow that had been accelerated by up to 5%. The anemometers on the *Polarstern* were unusual in that they were mounted on a mast held forward of the ship, 12 m upwind of the bow, and the flow had been considerably decelerated. However, anemometers on research ships are most often sited on some form of mast in the bows of the ship. For the ships studied, such anemometers were generally between 0 and 10 m downwind of the bow tip, and experienced flows that had been decelerated by between 0% and 9% and displaced vertically by between 0.5 and 1.5 m, with the larger displacements occurring for ships with a larger bow (e.g., the *James Clark Ross*) and vice versa (e.g., the *Suroit* and the *Challenger*). The magnitude of the deceleration of the flow will depend on (i) the proximity of the mast to the superstructure of the ship, (ii) the degree to which the superstructure presents a bluff obstacle to the flow (e.g., *Darwin*) rather than a more streamlined one (e.g., *Discovery*), (iii) the size and shape of the mast itself, and (iv) the proximity of the anemometer to any smaller-scale local obstructions. In general, instruments should be located as far forwards and as high above the deck as possible.

8. The impact of flow distortion on the measured C_{D10N}

For a ''typical'' anemometer mounted on a bow mast at a height of 18 m say, a reduction in the speed of the bow-on flow of 5% would cause the calculated U_{10N} value to be low by 5% and the C_{D10N} value to be overestimated by 12%. The effect on the resulting C_{D10N} to U_{10N} relationship would be an overestimate of the drag coefficient of 17% for a particular wind speed. If the flow is also displaced vertically by 1 m, the C_{D10N} estimate would be overestimated by a further 5%. Both aspects taken together produce a C_{D10N} to U_{10N} relationship that, for a given wind speed, will overestimate the C_{D10N} value by more than 20%.

Of the three ships modeled for bow-on flows with different incident wind speeds, none showed significant variation of the absolute wind speed error (section 6, Table 5). The anemometer sites examined on the *Darwin* and the *James Clark Ross* also showed little variation of the vertical displacement of the flow with incident wind speed. The largest variation in Δz was found for the foremast site on the *Discovery*, with a value of 1.1 m found for a 14 m s^{-1} bow-on flow and 0.7 m for a 20 m s^{-1} flow. Application of a Δz correction of 1.1 m for all wind speeds would result in a 2% underestimate in the C_{D10N} estimate for a U_{10N} of 20 m s^{-1}, and this underestimate would probably increase with increasing wind speeds. Conversely, the model for a 6 m s^{-1} flow suggested a Δz estimate of 1.4 m: in this case the application of a value of 1.1 m would result in a 1.5% overestimate in the C_{D10N} estimate at low wind speeds. It can therefore be seen that, although these errors are small, the use of a constant Δz estimate would result in an overall decrease in the slope of the calculated C_{D10N} to U_{10N} relationship.

Although it has been shown that the flow distortion and the resulting impact on the calculated C_{D10N} varies only slightly with the speed of the flow, the opposite has been found for the dependence of flow distortion with relative wind direction. For the extreme example of a beam-on flow, the same ''typical'' anemometer may experience flows that have been displaced by 5 m, for example, and the uncorrected C_{D10N} would therefore overestimate by about 25%. The limited amount of beam-on data available (Table 4) suggest that the flow may be accelerated to some extent. This would lead to an underestimate in C_{D10N}. The overall bias in the C_{D10N} to U_{10N} relationship would depend on the balance of the two effects. For example, if the flow was accelerated by 5%, the overall bias in the relationship would be reduced to an overestimate of the drag coefficient of 8% for a particular wind speed.

It should also be noted that quite small changes in the relative wind direction will also have a significant impact on the calculated C_{D10N}. For example, Table 4 lists the effects of flow distortion at anemometer sites on two ships for flows at 30° and 15° off the bow as well as for bow-on flows. Taking the mean of the various foremast anemometer sites on the *Discovery* as an example, the vertical displacement of the flow is 1.1 m for bow-on flows increasing to 1.4 m for a flow at $-15°$ and to 1.7 m for a flow at $-30°$ (the variation is not symmetrical about the bow since the anemometers were not located on the centerline of the ship). This would lead to an overestimate of about 3% in the $-30°$ C_{D10N} compared to the bow-on C_{D10N} data. Similarly, the error in the wind speed varies from -0.5% at 0° to $+2.5\%$ at $-30°$, leading to a mean C_{D10N} to U_{10N} relationship that would be biased low by about 10% for $-30°$ data compared to bow-on data. It can be seen from the table that the variation in the flow distortion effects used in this example are quite modest. Other anemometer sites show more significant variation for the same 30° change in the relative wind direction. It is interesting to note that the change in flow distortion with change of 30° in the wind direction is significant, even thought the tilt of the flow to the horizontal at the *Discovery* foremast sonic anemometer site, for example, varied by only 1° according to the model and less than 1° in the in situ results. For this reason it is thought that the angle of the flow to the horizontal is not a particularly sensitive measure of the flow distortion or of its variation.

In summary, the results from a model of the flow at a particular angle should only be applied to data from a rather narrow range of wind directions. For example, model results for a bow-on flow should not be assumed to apply to data obtained at wind directions of more than 10° or 15° from the bow (cf. Hare et al. 1999). For a particular set of data from a particular ship, it may be found that the application of such a correction may result in a C_{D10N} to U_{10N} relationship for data obtained at 30°, say, which is ''correct'' in the mean, but this may be due to the effect of the change in the wind speed error canceling the corresponding change in the vertical displacement. In other words, although the error in C_{D10N} may be offset by the error in U_{10N}, the friction velocity u_* may still be biased.

As pointed out by YT98, the behavior of a ship at sea depends on the conditions encountered. For example, the arrival of a large swell at an angle to a persistent strong wind would cause a ship that had previously been hove-to with the flow on to the bow to change its heading in order to balance the effects of wind and swell. This would result in the relative wind direction moving off the bow. It is therefore crucial to use the appropriate flow distortion corrections for the relative wind directions encountered. If this is not done, then a spurious signal in the flux data could be mistakenly associated with the change in the sea state.

It should be noted that, as demonstrated by DGH, the effects of flow distortion are also crucial to the measured sensible and latent heat fluxes. These authors show that, although the transfer coefficients for these fluxes are less sensitive than C_{D10N} to the wind speed error, they are more sensitive to the magnitude of the vertical displacement of the flow.

9. Conclusions

The results of this study have shown that CFD model simulations of the flow over research ships provide accurate estimates of the error in the speed of the mean flow to anemometer sites. Except for the cases where the anemometers were situated in the wake of an upstream obstacle, the modeled errors generally agreed with the in situ data to within 2%. These wind speed errors were seen to have no significant dependence on the incident wind speed.

This confidence in the modeled wind speeds allowed us to test the validity of the model estimate of Δz, the vertical displacement of the flow. This was done by comparing the drag coefficient to wind speed relationship obtained from the in situ data for flows at different relative wind directions. In order to examine the maximum impact of the vertical displacement correction, the comparison was made between bow-on flows where the vertical displacement was at a minimum (1 or 1.6 m), and beam-on flows where the vertical displacement increased to a maximum of 4 or 5 m, for the OWS *Cumulus* and the RRS *James Clark Ross*, respectively. The results showed that the estimate of the vertical displacement was relatively robust for bow-on flows, with typical Δz values of about 1 m for the ships studied. It should be emphasised that the uncertainty about the appropriate Δz value is insignificant for bow-on flows since, for most ships, the majority of the displacement takes place within 2 s of the flow reaching the anemometer site. The exception was for the anemometer situated above the superstructure of the *Cumulus*, where 0.4 m of the total 1.1 m displacement took place more than 2 s upstream: given the anemometer height of more than 23 m above sea level, this has a trivial impact on the calculated momentum flux. For the extreme case of beam-on flows there may be a small degree of uncertainly in the appropriate Δz estimate. However, this uncertainty amounts to only 25% at most (e.g., 4 m vs 5 m), which translates to a 5% uncertainty in the calculated C_{D10N} values. In other words, application of either Δz estimate (the full or the 2 s) is preferable to using a constant value of, say 1 m, regardless of the wind direction. In practice, most in situ data are obtained when the relative wind direction is on the bow, and can be corrected for flow distortion with some confidence.

For a bow-on flow to a typical anemometer site the effects of flow distortion result in a bias of the C_{D10N} estimate of more than 20%. However, this will vary depending on the shape of the ship and the exact anemometer location: biases of up to 60% in C_{D10N} have been seen. As a general rule, anemometers should be located as far forward and as high above the deck as possible. It has been shown that the effects of flow distortion are sensitive to the relative wind direction. For this reason data obtained when the wind is at an angle of more than about 10° from the modeled relative wind direction should either be discarded or additional models using the different wind directions should be made. Similar care should be taken when correcting the measured heat fluxes (DGH).

A final point to note is that flow distortion has a significant impact on the measured fluxes regardless of whether they are obtained via the inertial dissipation method or from the eddy correlation method. Although the eddy correlation measurements of the fluxes are not directly affected by the vertical displacement of the flow, they are severely affected by the impact of flow distortion on the turbulence itself (Oost et al. 1994): this aspect cannot be modeled using the methods described in this paper. In addition, both methods are affected by the error in the mean wind speed if the flux estimates are related to the wind speed via a transfer coefficient.

Acknowledgments. The authors are grateful for the long-term support and encouragement received from Dr. Peter K. Taylor (SOC, United Kingdom) and Dr. Val Swail (AES, Canada). This work has received funding from many sources: the OWS *Cumulus* was modeled as part of the NERC/DERA Joint Grant Funding project ''COOWS''; the Atmospheric Environment Service (AES), Canada, supported the modeling of the CSS *Hudson*; the ''ARCICE'' Grant GST/03/2205 from the U.K. Natural Environment Research Council supported the modeling of the RRS *James Clark Ross*; the R/V *Knorr* was supported by funds from the University of Kiel (Germany), Bedford Institute of Oceanography (Canada), NOAA, and the Naval Postgraduate School; and the R/V *Ronald H. Brown* model was supported by funds from the Woods Hole Oceanographic Institute. SOC participation on the *James Clark Ross* cruise in the autumn of 2000 was partially supported by the MAST project ''AutoFlux'' (MAS3-CT97-0108).

REFERENCES

Allen, J. T., and T. H. Guymer, 1997: RRS ''Discovery'' Cruise 224, Leg 1, 27 Nov–29 Dec 1996. OMEGA: Observations and Modeling of Eddy scale Geostrophic and Ageostrophic motion: Physical and biological observations in the eastern Alboran Sea (western Mediterranean). SOC Cruise Rep. 14, Southampton Oceanography Centre, United Kingdom, 92 pp.

Bacon, S., and M. J. Yelland, 2000: RRS ''James Clark Ross'' Cruise 44, 23 Jul–31 Aug 1999. Circulation and thermohaline structure—Mixing, ice and ocean weather CATS-MIAOW. SOC Cruise Rep. 33, Southampton Oceanography Centre, United Kingdom, 140 pp.

Berry, D. I., B. I. Moat, and M. J. Yelland, 2001a: Airflow distortion

at instrument sites on the *FS Polarstern.* SOC Internal Document 69, Southampton Oceanography Centre, United Kingdom, 36 pp.
——, ——, and ——, 2001b: Airflow distortion at instrument sites on the *RRS Challenger.* SOC Internal Document 70, Southampton Oceanography Centre, United Kingdom, 19 pp.
——, ——,and ——, 2001c: Airflow distortion at instrument sites on the *RRS James Clark Ross.* SOC Internal Document 75, Southampton Oceanography Centre, United Kingdom, 111 pp.
Birch, K. G., and R. W. Pascal, 1987: A meteorological system for research applications–MultiMet. *Proc. Fifth Int. Conf. on Electronics for Ocean Technology,* Edinburgh, United Kingdom, Institute of Electronic and Radio Engineers, IERE Publication 72, 7–12.
Blanc, T. V., 1986: Superstructure flow distortion corrections for wind speed and direction measurements made from Tarawa Class (LHA1-LHA5) ships. NRL Rep. 9005, 20 pp. [Available from Naval Research Laboratory, Washington, DC 20375-5000.]
——, 1987: Superstructure flow distortion corrections for wind speed and direction measurements made from Virginia Class (CGN38–CGN41) ships. NRL Rep. 9026, 24 pp. [Available from Naval Research Laboratory, Washington, DC 20375-5000.]
Castro, I. P., and A. G. Robins, 1977: The flow around a surface-mounted cube in uniform and turbulent streams. *J. Fluid Mech.,* **79,** 307–335.
Dobson, F. W., 1981: Review of reference height for and averaging time of surface wind measurements at sea. Marine Meteorology and Related Oceanographic Activities 3, World Meteorological Organisation, Geneva, Switzerland, 64 pp.
Dupuis, H., C. Guerin, D. Hauser, A. Weill, P. Nacass, W. Drennan, S. Cloche, and H. Graber, 2002: Impact of flow distortion corrections on turbulent fluxes estimated by the inertial dissipation method during the FETCH experiment on R/V *L'Atalante. J. Geophys. Res.,* in press.
Edson, J. B., C. W. Fairall, P. G. Mestayer, and S. E. Larsen, 1991: A study of the inertial-dissipation method for computing air–sea fluxes. *J. Geophys. Res.,* **96** (C6), 10 689–10 711.
Femsys, Ltd., 1999: FEMGV user manual. Femsys Ltd., Leicester, United Kingdom, 598 pp. [Available from Femsys Ltd., 158 Upper New Walk, Leicester LE1 7QA, United Kingdom.]
Hare, J. E., P. O. G. Persson, C. W. Fairall, and J. B. Edson, 1999: Behavior of Charnock's relationship for high wind conditions. Preprints, *13th Conf. on Boundary Layers and Turbulence,* Dallas, TX, Amer. Meteor. Soc., 252–255.
Henjes, K., 1996: Isotropic and anisotropic correlations in turbulent wind speed data. *Bound.-Layer Meteor.,* **84,** 149–167.
Hunt, J. C. R., 1973: A theory of turbulent flow round two-dimensional bluff bodies. *J. Fluid Mech.,* **61,** 625–706.
Kahma, K. K., and M. Leppäranta, 1981: On errors in wind speed observations on R/V *Aranda. Geophysica,* **17,** 155–165.
Launder, B. E., and B. Spalding, 1974: The numerical computation of turbulent flows. *Comp. Methods Appl. Mech. Eng.,* **3,** 269–289.
Leach, H., and R. T. Pollard, 1998: RRS ''Discovery'' Cruise 223, 28 Sep–19 Nov 1996. SOC Cruise Rep. 17, VIVALDI '96, Southampton Oceanography Centre, United Kingdom, 68 pp.
Moat, B. I., and M. J. Yelland, 1996a: Airflow over *Le Suroit* using the computational fluid dynamics package VECTIS. SOC Internal Document 3, Southampton Oceanography Centre, United Kingdom, 24 pp.
——, and ——, 1996b: Airflow over the *RRS Charles Darwin:* The disturbance of the flow at the anemometer sites used during cruises CD43 and CD98. SOC Internal Document 5, Southampton Oceanography Centre, United Kingdom, 41 pp.
——, and ——, 1996c: Airflow over the *RRS Discovery:* Variation of velocity errors with wind speed. SOC Internal Document 4, Southampton Oceanography Centre, United Kingdom, 26 pp.
——, and ——, 1997: Airflow distortion at anemometer sites on the *OWS Cumulus.* Southampton Oceanography Centre, United Kingdom, 22 pp. (Available from Southampton Oceanography Centre, Empress Dock, Southampton SO14 3ZH, United Kingdom).
——, and ——, 1998: Airflow distortion at instrument sites on the *RV Knorr.* Southampton Oceanography Centre, United Kingdom, 29 pp. (Available from Southampton Oceanography Centre, Empress Dock, Southampton SO14 3ZH, United Kingdom).
——, and ——, 2001: Airflow over the *RRS Discovery:* The variation of velocity errors with relative wind direction for anemometers mounted on VIVALDI cruise D223 and OMEGA cruise D224. SOC Internal Document 71, Southampton Oceanography Centre, United Kingdom, 107 pp.
——, D. I. Berry, and M. J. Yelland, 2001: Airflow distortion at instrument sites on the *RV Ronald H. Brown.* SOC Internal Document 66, Southampton Oceanography Centre, United Kingdom, 26 pp.
Oost, W. A., C. W. Fairall, J. B. Edson, S. D. Smith, R. J. Anderson, J. A. B. Wills, K. B. Katsaros, and J. DeCosmo, 1994: Flow distortion calculations and their application in HEXMAX. *J. Atmos. Oceanic Technol.,* **11,** 366–386.
Ricardo Consulting, 2001: VECTIS computational fluid dynamics (release 3.5) user's guide. Ricardo Consulting Engineers Ltd., Shoreham-by-Sea, United Kingdom, 262 pp. [Available from Ricardo Consulting Engineers Ltd., Bridge works, Shoreham-by-Sea, West Sussex BN43 5FG, United Kingdom.]
Surry, D., R. T. Edey, and I. S. Murley, 1989: Speed and direction correction factors for shipborne anemometers. Engineering Science Research Rep. BLWT-SS9-89, University of Western Ontario, London, ON, Canada, 83 pp.
Taylor, P. K., and M. J. Yelland, 2000: On the apparent ''imbalance'' term in the turbulent kinetic energy budget. *J. Atmos. Oceanic Technol.,* **17,** 82–89.
Thiebaux, M. L., 1990: Wind tunnel experiments to determine correction functions for shipborne anemometers. Canadian Contractor Rep. 36, Hydrography and Ocean Sciences, Bedford Institute of Oceanography, Dartmouth, NS, Canada, 57 pp.
Versteeg, H. K., and W. Malalasekera, 1999: *An Introduction to Computational Fluid Dynamics: The Finite Volume Method.* Longman, 257 pp.
Wucknitz, J., 1980: Flow distortion by supporting structures. *Air–Sea Interaction Instruments and Methods,* F. Dobson, L. Hasse, and R. Davis, Eds., Plenum Press, 605–626.
Yelland, M. J., and R. W. Pascal, 2000: RRS ''James Clark Ross'' Cruise, 11 Sep–17 Oct 2000. AutoFlux trials cruise, UK to Falklands Passage. SOC Cruise Rep. 32, Southampton Oceanography Centre, United Kingdom, 36 pp.
——, B. I. Moat, P. K. Taylor, R. W. Pascal, J. Hutchings, and V. C. Cornell, 1998: Wind stress measurements from the open ocean corrected for air-flow distortion by the ship. *J. Phys. Oceanogr.,* **28,** 1511–1526.